European Journal of Medicinal Chemistry 252 (2023) 115293

Contents lists available at ScienceDirect

European Journal of Medicinal Chemistry

journal homepage: www.elsevier.com/locate/ejmech

Research paper

Fatty acids as molecular carriers in cleavable antifungal conjugates

Michał Nowak [a,*], Andrzej S. Skwarecki [b], Joanna Pilch [b], Justyna Górska [b], Piotr Szweda [b], Maria J. Milewska [a], Sławomir Milewski [b]

[a] Department of Organic Chemistry, Faculty of Chemistry, Gdańsk University of Technology, 11/12 Narutowicza St., 80-233, Gdańsk, Poland
[b] Department of Pharmaceutical Technology and Biochemistry, Faculty of Chemistry, Gdańsk University of Technology, 11/12 Narutowicza St., 80-233, Gdańsk, Poland

ARTICLE INFO

Keywords:
Antifungal conjugates
5-Fluorocytosine
Trimethyl lock
Fatty acids

ABSTRACT

Conjugates composed of $C_{2\text{-}18}$ fatty acid (FA) residues as a molecular carrier and 5-fluorocytosine (5-FC) as an active agent, released upon the action of intracellular esterases on the ester bond between FA and "trimethyl lock" intramolecular linker, demonstrate good *in vitro* activity against human pathogenic yeasts of *Candida* spp. The minimal inhibitory concentrations (MIC) values for the most active conjugates containing caprylic (C_8), capric (C_{10}), lauric (C_{12}), or myristic (C_{14}) acid residues were in the 2–64 μg mL^{-1} range, except for these against the least susceptible *Candida krusei*. The least active conjugates containing C_2, C_{16}, or C_{18} FA were slowly hydrolyzed by esterase and probably poorly taken up by *Candida* cells, as found for their analogs containing a fluorescent label, Nap-NH_2 instead of 5-FC.

1. Introduction

Microbial resistance to chemotherapeutics has emerged and its spread worldwide resulted in substantial challenges for antimicrobial chemotherapy and significant threats to public health [1,2]. One of these threats is caused by human pathogenic fungi. During the past 20 years, the incidence of invasive fungal infections such as candidiasis, cryptococcosis, and aspergillosis in humans, especially in immunocompromised patients, has increased considerably [3]. In the past few years, fungal diseases caused an estimated over 1.6 million deaths annually diseases [4]. The current repertoire of antifungal chemotherapeutics is limited to azole derivatives (e.g., fluconazole and voriconazole), polyene macrolide antibiotic Amphotericin B, and candins (e.g., caspofungin and anidulafungin). Each of these treatment options has several drawbacks, such as drug-related toxicity, the emergence of resistant strains, nonoptimal pharmacokinetics, or poor solubility [5]. Therefore, there is a pressing need to discover new antifungal agents. An interesting option could be the exploitation of known inhibitors of enzymes catalyzing reactions of crucial importance for fungal growth and virulence, which are absent in mammalian cells. Selective inhibitors of such fungal enzymes could give rise to novel antifungal agents exhibiting selective toxicity against human pathogenic fungi. However, some inhibitors of fungal intracellular enzymes identified as potential targets, exhibit poor cellular penetration, due to their high hydrophilicity. One of the most promising strategies for overcoming this problem, is the use of molecular carriers, easily penetrating the fungal cell membrane to ensure delivery of an inhibitor to the target site. The so-called "Trojan horse" strategy is based on the idea of conjugation of any active substance with an appropriate molecular carrier. Once the conjugate is internalized, it should be cleaved intracellularly and the released active component can reach its target [6].

The known molecular carriers enter the cells by simple diffusion (some of the small cell-penetrating peptides - CPPs, carbon nanotubes, and terpenoid derivatives), are internalized by endocytosis (dendrimers and large CPPs), or take advantage of specific transport systems operating in microorganisms (siderophores and oligopeptides) [7]. Another possibility for molecular carriers ensuring internalization of a molecular carrier:inhibitor conjugate by simple diffusion could be fatty acid (FA) residues, which should provide a "lipophilicity input" to the conjugate, facilitating its translocation through the cell membrane. This option has

Abbreviations: 5-FC, 5-fluorocytosine; DCC, dicyclohexylcarbodiimide; DCM, dichloromethane; DEPBT, 3-(diethoxyphosphoryloxy)-1,2,3-benzotriazin-4(3H)-one; DIPEA, *N,N*-diisopropylethylamine; DMAP, 4-dimethylaminopyridine; DMF, dimethylformamide; DMSO, dimethylsulfoxide; EH_{50}, concentration causing lysis of 50% of erythrocytes; FA, fatty acid; MIC, minimum inhibitory concentration; MS, mass spectrum; Nap-NH_2, *N*-butyl-4-aminoethyl-1,8-naphtalimide; NHS, *N*-hydroxysuccinimide; MOPS, 3-(*N*-morpholino)propanesulfonic acid; PCC, pyridinium chlorochromate; RBC, red blood cells; THF, tetrahydrofuran; TML, trimethyl lock.

* Corresponding author.
E-mail address: michal.nowak1@pg.edu.pl (M. Nowak).

https://doi.org/10.1016/j.ejmech.2023.115293
Received 29 August 2022; Received in revised form 15 March 2023; Accepted 15 March 2023
Available online 17 March 2023

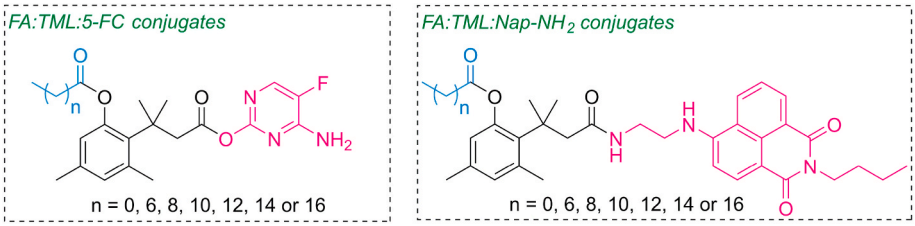

Fig. 1. Chemical structures of FA:TML:5-FC and FA:TML:Nap-NH_2 conjugates.

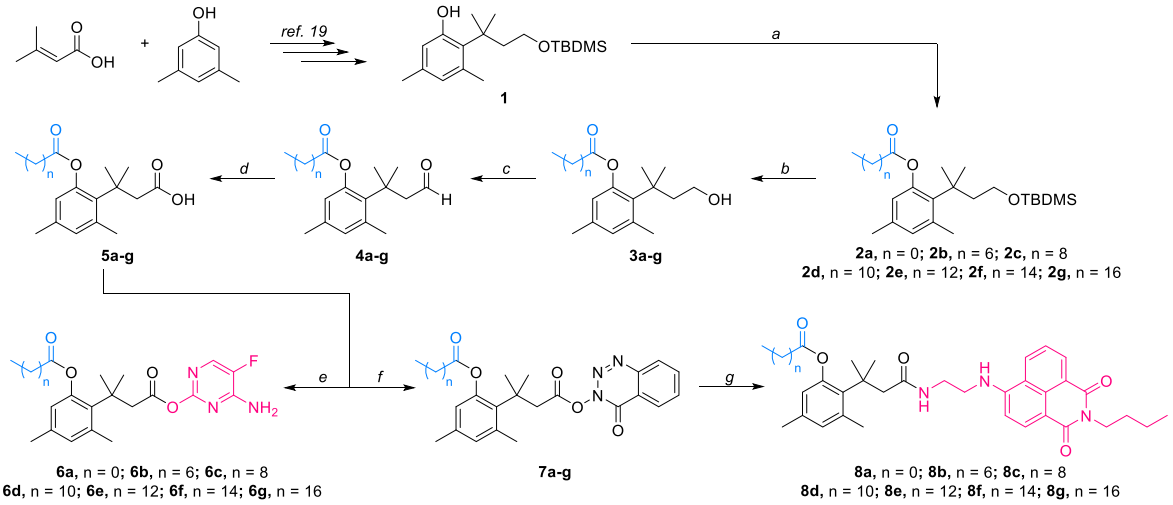

Scheme 1. Synthesis of FA:TML:5-FC (**6a-g**) and FA:TML:Nap-NH_2 (**8a-g**) conjugates. Reaction conditions: a) carboxylic acid (1.5 equiv.), DCC (2 equiv.), DMAP (0.7 equiv.), DCM, rt, overnight; b) THF/H_2O/AcOH, (1/1/3, v/v/v), rt, 2 h; c) PCC (2 equiv.), DCM, Ar, rt, 3 h; d) $NaClO_2$ (4.8 equiv.), NaH_2PO_4 (1.2 equiv.), 2-methylbut-2-ene (20 equiv.), acetone/tertBuOH/H_2O (6/4/1, v/v/v), rt, overnight; e) i. $(COCl)_2$ (1.5 equiv.), DMF (0.14 equiv.), DCM, 0.5 h at 0 °C, then 2 h at rt; ii. 5-fluorocytosine (0.9 equiv.), DMAP (0.2 equiv.), Py (1.4 equiv.), DCM, 0.5 h at 0 °C, then 2 h at rt; f) DEPBT (2 equiv.), DIPEA (4 equiv.), DMF, rt, 5 h; g) **Nap-NH_2** (1.1 equiv.), DIPEA (3 equiv.), DMF, rt, 4 h.

been recently exploited for the construction of non-cleavable conjugates of quinolone drugs, demonstrating antibacterial and anticancer activity [8] but any cleavable FA-containing conjugates have not been reported yet.

Here, we propose a novel version of the "Trojan horse" approach to the construction of enzymatically cleavable conjugates composed of FA residue as a nanocarrier and 5-fluorocytosine (5-FC) as a "warhead", released upon the action of intracellular esterases on the ester bond between FA and the "trimethyl lock" (TML) intramolecular linker. 5-FC, chosen as a warhead molecule in this study, is a well-known antifungal agent. The mechanism of its antifungal action comprises internalization by cytosine permease and conversion into 5-fluorouracil by cytosine deaminase. The finally formed 5-fluorouridine monophosphate and 5-fluoro-2′deoxyuridylate inhibit RNA and DNA biosynthesis, respectively. The selective toxicity of 5-FC in the fungi:mammals system is due to the absence of cytosine deaminase in mammalian cells [9]. Because of the high occurrence of resistance to this antifungal [10], 5-FC is not used in monotherapy and should always be combined with another antifungal, usually an azole or polyene drug [11]. Mechanisms of fungal resistance to 5-FC are of multiple character [12] but one of them is based on the consequences of mutations in the *FCY2* gene encoding cytosine permease, resulting in inefficient drug uptake by fungal cells [13].

The TML linker employed in our constructs, based on the trimethyl substituted *o*-hydroxycinnamic acid residue, is *O*-acylated with FA, while a warhead residue, 5-FC, or a fluorescent label, Nap-NH_2, is linked to TML through an ester or amide bond, respectively. This linker was previously employed in different triggering versions in several prodrug constructs [14,15], very few antibacterials [16–18] but not in antifungals. In the case of our FA:TML:warhead conjugates, it was assumed that enzymatic hydrolysis of the FA-TML ester bond should trigger lactonization of the TML system, involving the release of the warhead.

2. Results and discussion

2.1. Chemistry

Seven conjugates of 5-FC with FA nanocarriers, containing 2–18 carbon atoms, linked through the TML system (FA:TML:5-FC) and their analogs containing a fluorescent probe, Nap-NH_2, instead of 5-FC (FA:TML:Nap-NH_2), shown in Fig. 1 were synthesized and characterized.

The synthetic route leading to the final preparation of conjugates is shown in Scheme 1. Precursor **1** of the TML system was obtained similarly as described in our previous work [19], starting from the commercially available 3-methylbut-2-enoic acid and 3,5-dimethylphenol. The resulting *O*-protected phenol **1** was acylated with one of the seven different non-branched and saturated carboxylic acid residues, *i.e.* acetic (C_2), caprylic (C_8), capric (C_{10}), lauric (C_{12}), myristic (C_{14}), palmitic (C_{16}), or stearic (C_{18}) acid. The acylation reactions were accomplished by Steglich esterification, under coupling conditions of DCC and DMAP. The resulting esters **2a-g** were deprotected under mild acidic conditions of acetic acid and then the resulting alcohols **3a-g** were subjected to oxidation reaction with PCC, resulting in the formation of aldehydes **4a-g**, followed by Pinnick oxidation. The thus obtained carboxylic acids **5a-g** served as starting material for the preparation of final conjugates. The ones incorporating 5-FC were prepared by activation of the carboxyl moiety with oxalyl chloride/DMF mixture, leading to carboxyl chlorides, which were treated with 5-fluorocytosine, giving the target compounds **6a-g** as esters. To obtain fluorescent **Nap-NH_2**

Table 1
MIC values (μg mL^{-1}) of conjugates **6a-g** and 5-FC against reference strains of *Candida* spp.

Strains	Compounds							
	6a	6b	6c	6d	6e	6f	6g	5-FC
Candida albicans	16	8	8	8	4	16	128	1
Candida glabrata	8	2	4	4	2	8	32	0.5
Candida krusei	>512	128	256	256	512	>512	>512	>512
Candida pseudotropicalis	64	32	32	64	32	128	512	1
Candida guilliermondii	16	8	8	8	8	32	256	0.5
Candida rugosa	32	16	16	16	16	64	>512	2
Candida famata	8	4	8	4	4	16	256	1
Candida parapsilosis	4	4	4	4	4	8	128	2

derivatives carboxylic acids **6a-g** were first converted into 4-oxobenzo [*d*] [1–3]triazyn-3(4*H*)-yl esters **7a-g** by treating them with 3-(diethoxyphosphoryloxy)-1,2,3-benzotriazin-4(3*H*)-one (DEPBT) in a presence of a tertiary amine. Active esters **7a-g** then reacted with the primary amino group of **Nap-NH_2** in DMF, in a presence of a tertiary amine, which led to the formation of amides **8a-g.**

The analytical data of reaction products and important intermediates are presented as Supplementary information. Formation of an ester bond instead of an alternative amide in reaction carried out in DCM, is not surprising, since it was previously shown that the amino-hydroxy tautomer of 5-FC strongly dominates in inert matrixes, in sharp contrast with the dominance of the amino-oxo form in polar media [20].

2.2. Antifungal activity and hemotoxicity

Conjugates **6a-g** were tested for antifungal *in vitro* activity against eight representative strains of human pathogenic yeasts of Candida spp., including *C. albicans*, *C. glabrata*, and *C. parapsilosis* species, most frequently causing disseminated candidiases [21]. The MIC values were determined by the serial dilution microplate method, following the CLSI guidelines [22] 5-FC was employed as a reference compound. The results obtained are presented in Table 1.

All conjugates exhibited antifungal activity. Among the *Candida* spp. employed for MIC determination, the most susceptible were *C. glabrata,* and the least susceptible were *C. krusei* and *C. pseudotropicalis*. Comparing antifungal activity of conjugates **6a-g**, the least active appeared these with the longest FA residues, **6g** (C_{18}), **6f** (C_{16}), and the shortest one, **6a** (C_2). For the remaining conjugates, **6b** (C_8), **6c** (C_{10}), **6d** (C_{12}), and **6e** (C_{14}), the MIC values were very similar. Even the most active conjugates were less active than their component warhead, *i.e.* 5-FC, except for *Candida krusei*, apparently resistant to 5-FC but susceptible to conjugates **6b** – **6e**. This difference could be at least in part explained by the fact that in fungal cells, 5-FC is taken up by the active transport system operating against the concentration gradient (cytosine permease), so that the drug can be accumulated intracellularly up to the high concentration. Such accumulation is not possible in the case of conjugates, crossing the cell membrane by a simple diffusion, which is effective only up to the equalization of concentrations on both sides of the cytoplasmic membrane. The lowest susceptibility of *C. krusei*, both to 5-FC and the conjugates, is well understandable in light of the fact that in this microorganism resistance to 5-FC is very common [10], also due to the mutations in the *FCY2* gene.

It is known that the shorter chain FAs, especially caprylic (C_8) and lauric (C_{12}) acid, exhibit antifungal activity [23]. One may expect that these FAs are released from conjugates **6b** and **6d**, respectively, upon the action of intracellular fungal esterase, so that they could participate in the overall growth inhibitory effect. To exclude this possibility, we determined the antifungal *in vitro* activity of all FAs used for the construction of conjugates **6a-g**. No growth inhibitory effect was observed at concentrations up to 512 μg mL^{-1}.

All conjugates were tested for their potential hemotoxicity. Such effect could be possible, if conjugates containing FAs, especially their longer versions, affected the integrity of the cell membrane of red blood cells (RBC). However, in our hands none of the conjugates **6a-g**, at concentrations up to 200 μg mL^{-1} induced lysis of RBC (EH) at higher than 5% level. Taken as a positive control in this experiment the well-known antifungal antibiotic Amphotericin B, induced RBC lysis at low concentrations, and 50% hemolysis for this compound (EH_{50}) was noted at 3.46 ± 0.15 μg mL^{-1}.

2.3. Microscopic examination of uptake of FA:TML:florescent probe conjugates

Making sure that conjugates **6a-g** are not membrane-active compounds, it could be anticipated that their antifungal activity is due to the intracellular action of the warhead, *i.e.* 5-FC, which implicates the necessity of conjugate internalization. We were able to confirm such internalization for conjugates **8a-g**, structural analogs of **6a-g**, containing a florescent probe, Nap-NH_2 instead of 5-FC. Compounds **8a-g** did not demonstrate any antifungal *in vitro* activity up to 512 μg mL^{-1}. Microscopic examination of suspensions of *C. albicans* cells incubated with one of the compounds **8a-g** at 2 μg mL^{-1} for 1 h revealed differential fluorescent staining of cells, as shown in Fig. 2. The strongest fluorescence was noted in cells exposed to **8b**, weaker in cells treated with **8a**, **8c,** and **8d,** and the weakest, but still detectable, in **8f** and **8g** containing samples. The image of the Z-stack projection of cells treated with **8b**, shown in Fig. 3, demonstrates uniform fluorescent staining of cell interiors, thus indicating a cytoplasmic localization of the fluorescent probe. These results suggest the relatively fastest internalization of **8b** (C_8) and the slowest accumulation of **8f** (C_{16}) and **8g** (C_{18}). Such relations do not have to be directly related to 5-FC-containing counterparts of **8a-g**, *i.e.* compounds **6a-g**, but at least in part explain the differential antifungal activity of the latter.

The kinetics of **8b** uptake by *C. albicans*, *C. glabrata,* and *C. krusei* cells were determined in a semi-quantitative way. As shown in Fig. 4, the highest number of cells emitting green fluorescence after 10 and 30 incubation was observed for *C. glabrata* and the lowest for *C. krusei*. It may suggest the fastest accumulation of the fluorescent probe in the former cells and the slowest in the latter. Such relationship overlaps, probably not accidently, with differential susceptibility of the three *Candida* spp, to **6b**, *i.e.* the 5-FC-containing **8b** analogue and other FA:TML:5-FC conjugates.

2.4. Enzymatic cleavage of FA:TML:5-FC conjugates

Antifungal activity of FA:TML:5-FC conjugates may depend not only on the effectiveness of uptake but also on the velocity of their enzymatic cleavage. This feature of compounds **6a-g** was examined in the model reaction with pig liver esterase. The composition of samples collected at time intervals was analyzed by HPLC-DAD-MS. The results of these analyses are shown in Fig. 5.

The presence of signals attributed to lactone C in all chromatograms confirms that esterase cleaves the ester bond between FA and TML, thus inducing lactonization of TML, with concomitant release of 5-FC, as shown in Scheme 2. Formation of lactone C from TML is impossible if the phenolic hydroxyl is blocked but its release induces immediate fast

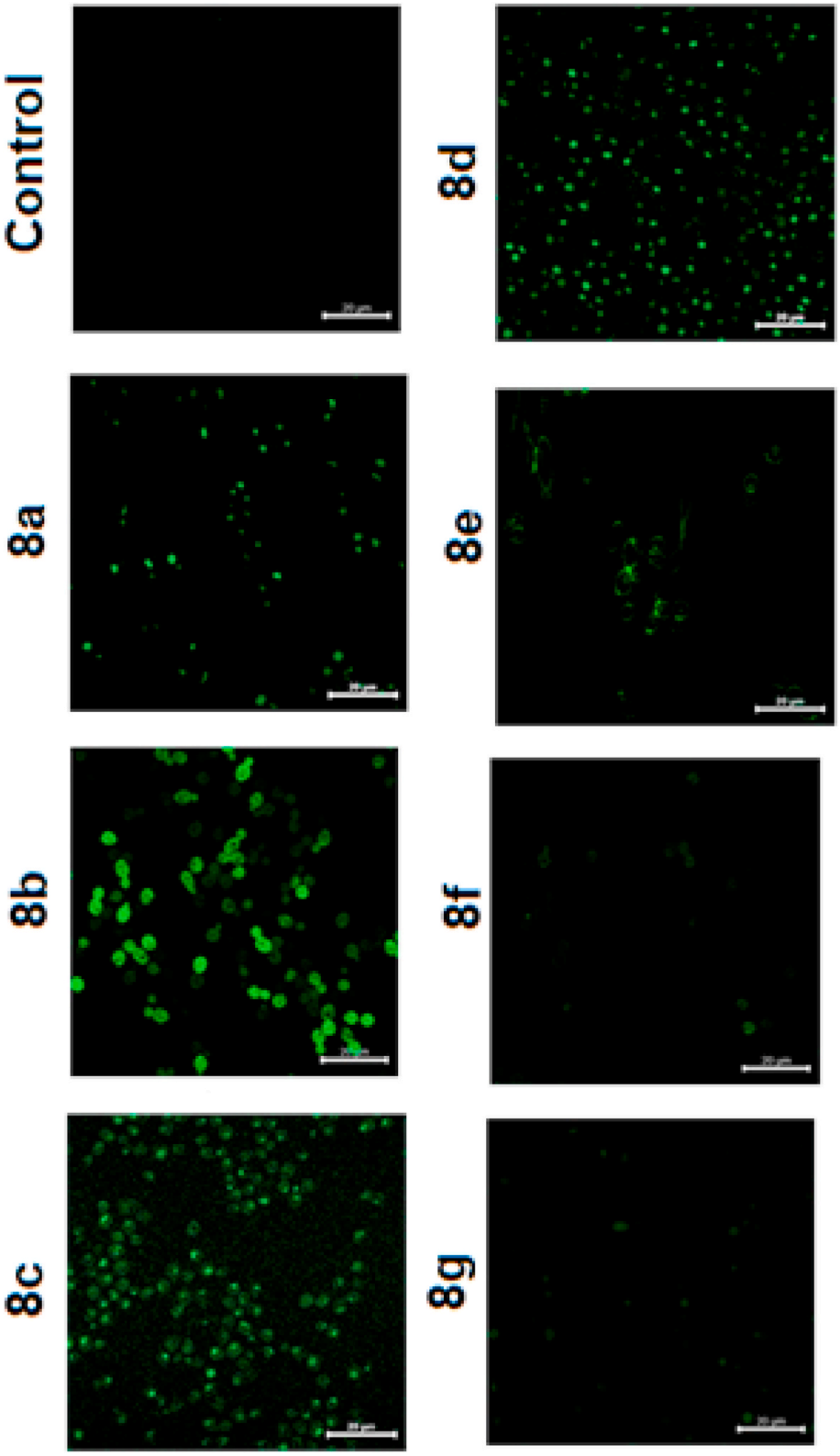

Fig. 2. Accumulation of fluorescent probes **8a-g** in *C. albicans* cells. Cell suspensions were incubated for 1 h with one of the compounds **8a-g** at 2 μg mL^{-1} and then the preparations prepared from collected cells were observed by fluorescent microscopy at λ_{exc} = 438 nm and λ_{em} = 527 nm.

lactonization [14].

$R_1 = CH_3\text{-}(CH_2)_n$; R_2XH = 5-FC

In all chromatograms presented in Fig. 5, the time-dependent decrease of signals derived from conjugates and respective increase of 5-FC peaks is observed. The rate of this conversion was slower for conjugates **6f** and **6g** and much faster for **6c**, **6d,** and **6e**. A possible lower rate of 5-FC release from **6f** and **6g**, may therefore contribute to the lower antifungal activity of these conjugates.

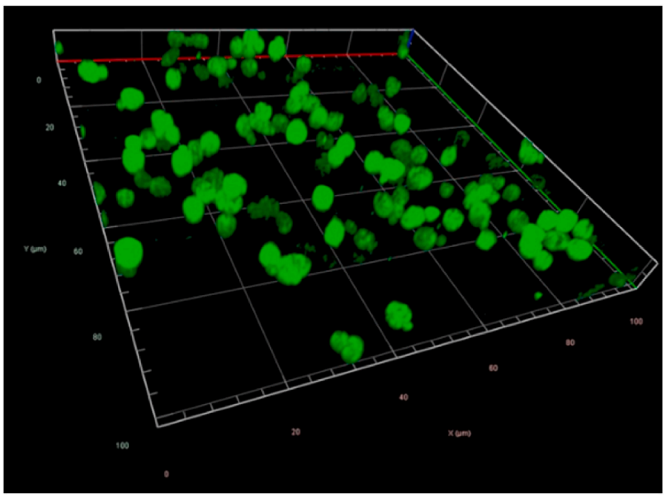

Fig. 3. Image of the Z-stack projection of *C. albicans* cells treated for 1 h with the fluorescent probe **8b**. Confocal microscopy at λ_{exc} = 438 nm and λ_{em} = 527 nm.

3. Conclusions

Properties of the FA:TML:5-FC conjugates presented in this work indicate that FA residues, particularly these of caprylic (C_8), capric (C_{10}), lauric (C_{12}), and myristic (C_{14}) acid, could be applied as molecular carriers for the construction of enzymatically cleavable conjugates demonstrating antifungal activity. The obvious advantage of FAs as candidates for molecular carriers is their very simple structure and in consequence, relative simplicity of conjugation. Nevertheless, the FA:TML:5-FC conjugates exhibit lower antifungal activity than 5-FC, except for that against *C. krusei*.. The previously described antimicrobial, peptidase cleavable conjugates based on oligopeptides as molecular carriers and amino acid-derived warheads, usually demonstrated higher antimicrobial activity than their constitutive warheads [24–27]. Nevertheless, the intrinsic activity of those warheads was very low, for their very poor uptake by microbial cells. In contrast, 5-FC is very effectively transported by fungal cytosine permease and in consequence, exhibits high antifungal activity. Paradoxically, this feature of 5-FC is also a reason for the high frequency of fungal resistance to this drug, resulting from mutations in the cytosine permease encoding *FCY2* gene. Such resistance to FA:TML:5-FC conjugates is not possible, since they are accumulated in fungal cells by simple diffusion.

This is worth mentioning, that although oligopeptidic and photo-triggered micelle-drug conjugates incorporating 5-fluorouracil are known [28,29], any congeners with 5-FC have not been described in the literature previously. In our hands, 5-FC was used as a tool to demonstrate usefulness of FAs as molecular carriers in TML-containing cleavable conjugates and to optimise their size (length). These results give rise to the construction of FA:TML:X conjugates, in which X would be any inhibitor of the intracellular microbial enzyme, not demonstrating intrinsic antimicrobial activity.

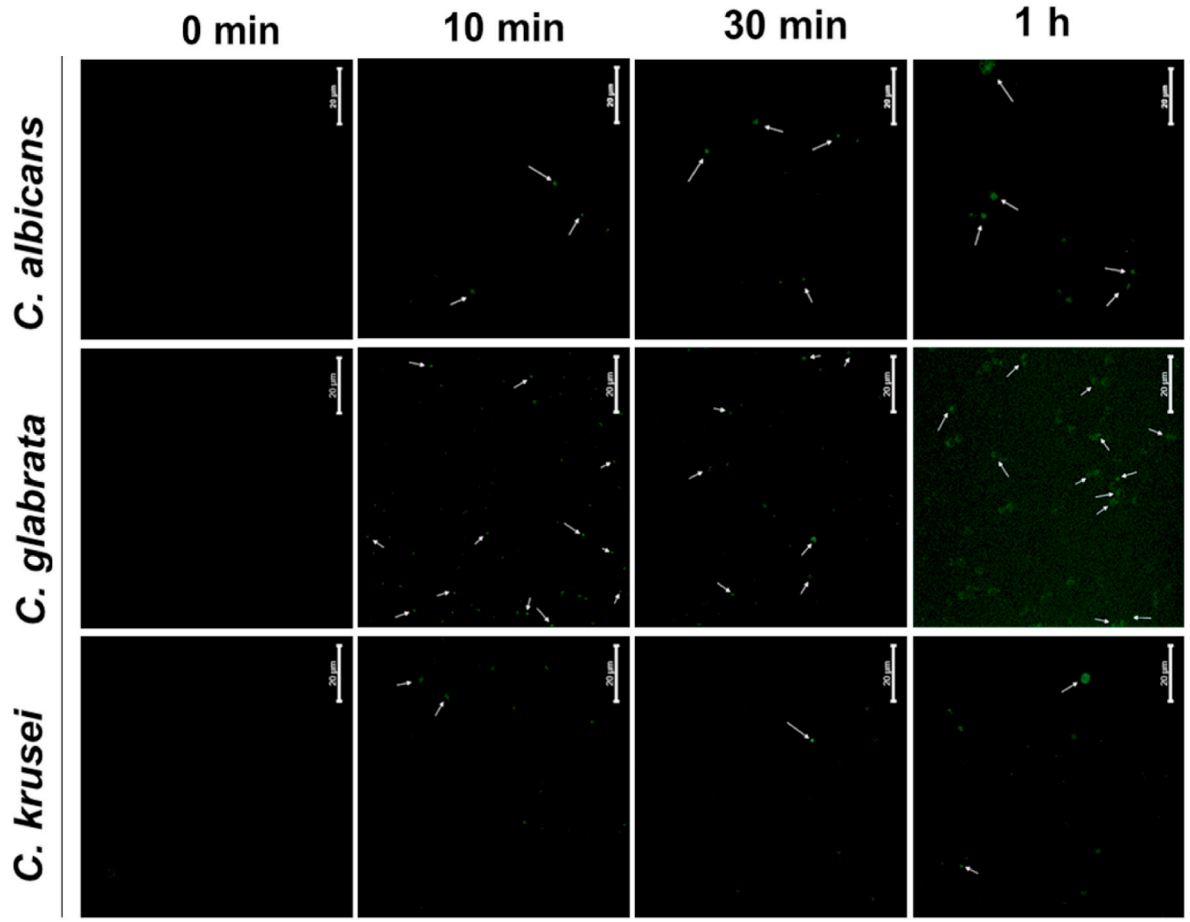

Fig. 4. Kinetics of **8b** uptake by *C. krusei*, *C. glabrata* and *C. albicans* cells. The arrows indicate cells exhibiting particularly intensive fluorescence. Fluorescence microscopy at λ_{exc} = 438 nm and λ_{em} = 527 nm.

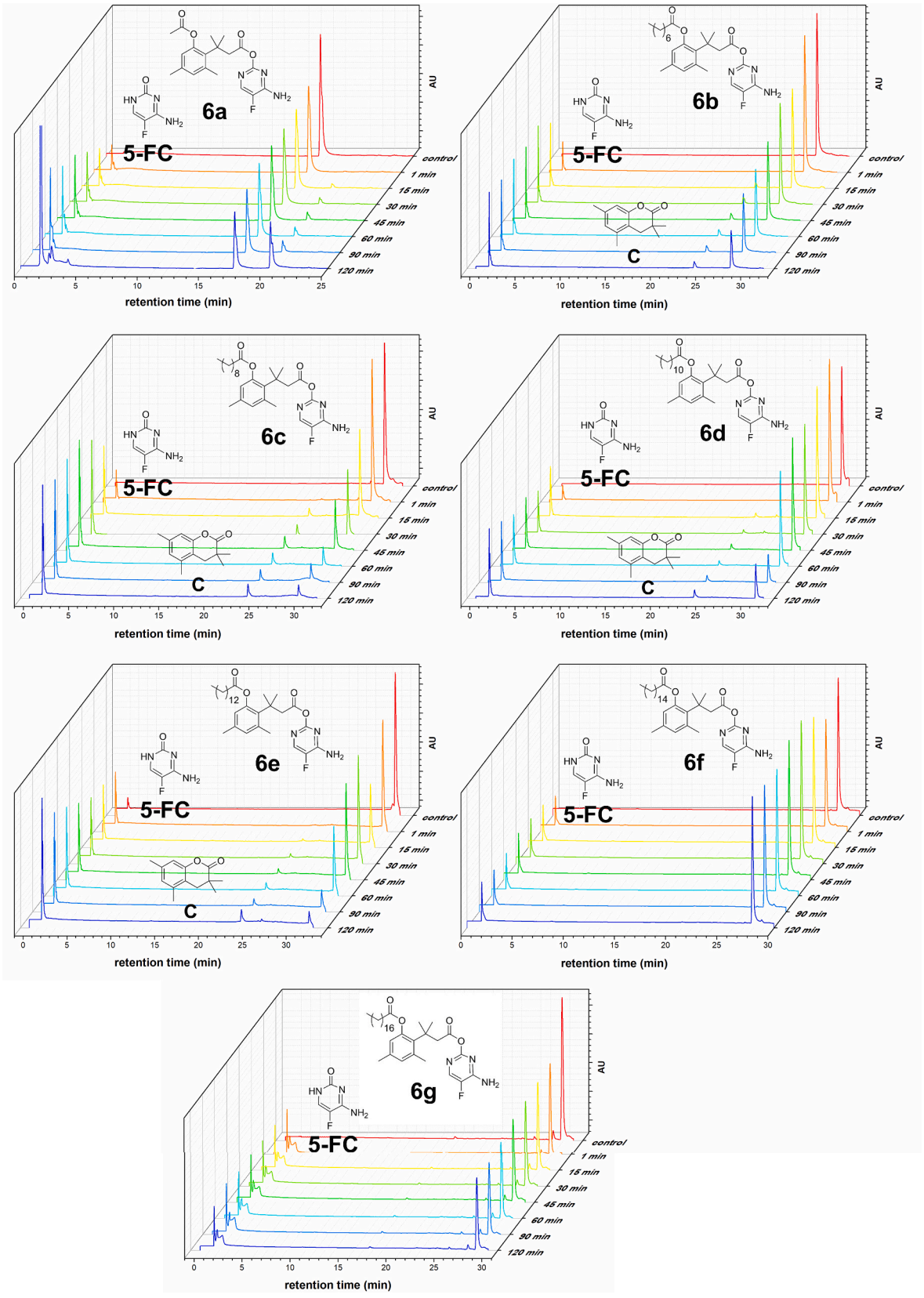

Fig. 5. Time-dependent cleavage of conjugates **6a-g** by pig liver esterase. Samples collected from incubation mixtures were analyzed by HPLC-DAD-MS. Absorbance was measured at $\lambda = 254$ nm. AU – arbitrary units.

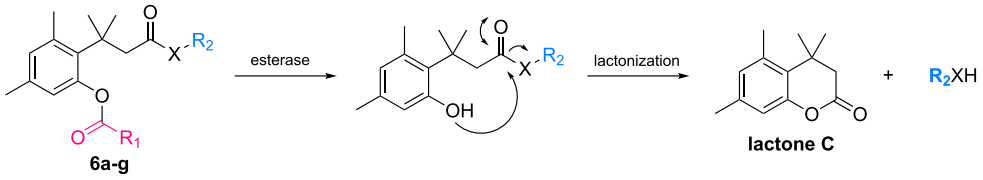

Scheme 2. Mechanism of esterase-triggered warhead release from conjugates **6a-g**.

4. Materials and methods

4.1. General

All solvents and reagents were used as obtained from commercial sources. ^{1}H NMR and ^{13}C NMR spectra were obtained at 500 MHz Varian Unity Plus spectrometer and the deuterated solvents were used as internal locks. HPLC-DAD-MS data was acquired using 1260 Infinity II and 6470 Triple Quad LC/MS system (Agilent Technologies). Column chromatography was performed with silica gel (0.040–0.063 mm) by using the indicated solvent systems. Automated flash chromatography was performed on CombiFlash Nextgen 300+ (Teledyne ISCO) system using RediSep Bronze silica gel column cartridges.

4.2. Syntheses

4.2.1. N-butyl-4-bromo-1,8-naphthalimide

A mixture of 1.00 g (3.61 mmol) of 4-bromo-1,8-naphthalic anhydride and 25 mL of acetic acid was heated to reflux under nitrogen atmosphere and then 1.1 mL (10.83 mmol) of *n*-butylamine was added dropwise. Once the addition was completed, the mixture was allowed to stir under reflux for 4 h. The mixture was cooled to room temperature ant then poured onto 100 mL of cold water. The resulted suspension was extracted with chloroform (3 × 75 mL) and then the organic layer was washed with 1 M $HCl_{(aq)}$ solution (2 × 75 mL), brine (75 mL), saturated solution of $NaHCO_{3(aq)}$ (3 × 75 mL) and brine (75 mL), respectively. The organic layer was dried under anhydrous $MgSO_4$, then the desiccant was filtered off and the filtrate was concentrated *in vacuo*. The brown solid residue was purified by column chromatography using the mixture of solvent hexanes/AcOEt, 7/3, v/v as a mobile phase, obtaining 1.06 g (3.19 mmol, 88%) of imide as a light-yellow solid. ^{1}H NMR (500 MHz, $CDCl_3$) δ: 8.65 (dd, 1H, J = 7.3, 0.9 Hz), 8.56 (dd, 1H, J = 7.3, 0.9 Hz), 8.42 (d, 1H, J = 7.8 Hz), 8.04 (d, 1H, J = 7.9 Hz), 7.85 (dd, 1H, J = 8.4 Hz, 7.4 Hz), 4.18 (m, 2H), 1.73 (quint, 2H, J = 7.5 Hz), 1.46 (m, 2H), 1.00 (t, 3H, J = 7.4 Hz). ^{13}C NMR (125 MHz, DMSO-d_6) δ: 163.18, 163.12, 132.89, 131.89, 131.70, 131.26, 130.09, 129.49, 129.13, 128.55, 123.03, 122.25, 29.87, 20.39, 14.06.

4.2.2. N-butyl-4-[(2-aminoetylo)amino]-1,8-naphthalimide (***Nap-NH$_2$***)

Ethylenediamine, 10 mL, was heated under anhydrous conditions to 60 °C and then 900 mg (2.71 mmol) of *N*-butyl-4-bromo-1,8-naphthalimide was added as a solid during 1.5 h. Subsequently, the mixture was allowed to stir at 60 °C for another 1.5 h and then was cooled to room temperature and poured onto 100 mL of cold water. The resulting suspension was extracted with chloroform (4 × 75 mL) and then the organic layer was washed with saturated $NaHCO_{3(aq)}$ (3 × 75 mL) and brine (75 mL), respectively. The organic layer was dried under anhydrous $MgSO_4$, the desiccant was filtered off and the filtrate was concentrated under reduced pressure. The orange solid residue was purified by column chromatography using the mixture of solvents $CHCl_3$/MeOH/H_2O, 65/10/2, v/v/v as a mobile phase, obtaining 740 mg (2.38 mmol, 88%) of Nap-NH_2 as a yellow solid. R_f 0.38 ($CHCl_3$/MeOH/H_2O, 65/10/2, v/v/v). ^{1}H NMR (500 MHz, DMSO-d_6) δ: 8.69 (d, 1H, J = 8.4 Hz), 8.41 (d, 1H, J = 7.2 Hz), 8.24 (d, 1H, J = 7.2 Hz), 7.65 (t, 1H, J = 7.7 Hz), 6.78 (d, 1H, J = 8.6 Hz), 3.99 (t, 2H), 3.35 (m, 3H), 2.86 (t, 2H, J = 6.5 Hz), 1.60 (m, 4H), 1.33 (m, 2H), 0.91 (t, 3H, J = 7.4 Hz). ^{13}C NMR (125 MHz, DMSO-d_6) δ: 164.15, 163.35, 151.09, 134.50, 130.88, 129.72, 128.98, 124.55, 122.29, 120.50, 108.02, 104.27, 46.61, 30.29, 20.29, 14.19.

2-{3-[(*O-tert*-butyldimethylsilyl)hydroxy]-1,1-dimethylpropyl}-3,5-dimethylphenol **1** was obtained according to the procedure previously reported [19].

4.2.3. 2-(3-hydroxy-1,1-dimethylpropyl}-O′-acyloyl-3,5-dimethylphenol (*3a-g*) – general procedure

A stirred mixture of 15.5 mmol of phenol **1**, 18.6 mmol of a carboxylic acid and 10.8 mmol of DMAP in dry DCM was cooled in an ice bath to 0 °C, and then 31 mmol of DCC dissolved in dry DCM was added dropwise. The mixture was stirred at room temperature overnight. The precipitate of DCU was filtered off and the filtrate was concentrated under reduced pressure. The residue was dissolved in ethyl acetate and washed with saturated $NaHCO_{3(aq)}$, 5% $NaHSO_{4(aq)}$ and water, respectively. The organic layer was dried over anhydrous $MgSO_4$, the desiccant was filtered off and the filtrate was concentrated under reduced pressure. The crude silyl ether was dissolved in a mixture of THF/H_2O/AcOH (1/1/3, v/v/v) and stirred at room temperature for 3 h. The solvent was evaporated under reduced pressure. The residue was dissolved in AcOEt and washed with water, saturated $NaHCO_{3(aq)}$ and water, respectively. The organic layer was dried over anhydrous $MgSO_4$, the desiccant was filtered off and the filtrate was concentrated under reduced pressure. The residue was purified by flash chromatography on silica gel, using a mixture of solvents hexanes/AcOEt (0% → 30%) as a mobile phase.

4.2.4. 2-(3-hydroxy-1,1-dimethylpropyl)-3,5-dimethylphenyl acetate ***3a***

Starting from 1.00 g (3.10 mmol) of phenol **1** and 220 mg (3.72 mmol) of acetic acid, 510 mg (2.04 mmol, 66%) of alcohol **3a** was obtained as a colourless oil.

^{1}H NMR (500 MHz, $CDCl_3$) δ: 6.85 (s, 1H), 6.58 (s, 1H), 3.55 (t, 2H, J = 7.3 Hz), 2.55 (s, 3H), 2.31 (s, 3H), 2.25 (s, 3H), 2.07 (2H, t, J = 7.4 Hz), 1.51 (s, 6H). ^{13}C NMR (125 MHz, $CDCl_3$) δ: 175.4, 154.4, 143.2, 141.0, 138.4, 137.3, 128.0, 65.3, 50.4, 43.8, 36.7, 30.1, 26.6, 24.9.

4.2.5. 2-(3-hydroxy-1,1-dimethylpropyl)-3,5-dimethylphenyl caprylate ***3b***

Starting from 5.00 g (15.5 mmol) of phenol **1** and 2.68 g (18.6 mmol) of caprylic acid, 3.1 g (9.27 mmol, 60%) of alcohol **3b** was obtained as a colourless oil.

^{1}H NMR (500 MHz, DMSO-d_6) δ: 6.82 (s, 1H), 6.55 (s, 1H), 4.25 (t, 1H, J = 5.0Hz), 3.20 (m, 2H), 2.54 (t, 2H, J = 7.4 Hz), 2.48 (s, 3H), 2.18 (s, 3H), 1.91 (t, 2H, J = 7.1 Hz), 1.63 (quint, 2H, J = 7.3 Hz), 1.39 (s, 6H), 1.37–1.22 (br, 8H) 0.88 (t, 3H, J = 7.1 Hz). ^{13}C NMR (125 MHz, DMSO-d_6) δ: 172.7, 150.1, 138.3, 135.7, 134.4, 132.1, 123.6, 58.7, 46.0, 39.0, 34.6, 32.0, 31.6, 28.9, 28.8, 25.3, 24.6, 22.5, 20.1, 14.4.

4.2.6. 2-(3-hydroxy-1,1-dimethylpropyl)-3,5-dimethylphenyl caprate ***3c***

Starting from 2.67 g (8.28 mmol) of phenol **1** and 2.1 g (12.2 mmol) of capric acid, 1.70 g (4.69 mmol, 57%) of alcohol **3c** was obtained as a colourless oil.

^{1}H NMR (500 MHz, DMSO-d_6) δ: 6.82 (s, 1H), 6.55 (s, 1H), 4.23 (t, 1H, J = 5.0 Hz), 3.21 (m, 2H), 2.54 (t, 2H, J = 5.8Hz), 2.48 (s, 3H), 2.18 (s, 3H), 1.91 (m, 2H), 1.63 (quint, 2H, J = 7.4 Hz), 1.39 (s, 6H), 1.36–1.22 Hz (br, 12H), 0.87 (t, 3H, J = 7.3 Hz). ^{13}C NMR (125 MHz, DMSO-d_6): δ: 172.6, 150.1, 138.3, 135.7, 134.4, 132.1, 123.6, 58.7,

46.0, 39.0, 34.6, 32.0, 31.8, 29.3, 29.2, 29.1, 28.9, 25.2, 24.6, 22.6, 20.1, 14.4.

*4.2.7. 2-(3-hydroxy-1,1-dimethylpropyl)-3,5-dimethylphenyl laurate **3d***

Starting from 2.00 g (6.20 mmol) of phenol **1** and 1.49 g (7.44 mmol) of lauric acid, 1.67 g (4.28 mmol, 69%) of alcohol **3d** was obtained as a colourless oil.

^{1}H NMR (500 MHz, DMSO-d_6) δ: 6.82 (s, 1H), 6.54 (s, 1H), 4.24 (br, 1H), 3.22 (m, 2H), 2.53 (t, 2H, J = 7.5 Hz), 2.48 (s, 3H), 2.17 (s, 3H), 1.92 (m, 2H), 1.63 (quint, 2H, J = 7.3 Hz), 1.40 (s, 6H), 1.38–1.20 Hz (br, 16H), 0.86 (t, 3H, J = 7.4 Hz). ^{13}C NMR (125 MHz, DMSO-d_6): 172.5, 150.1, 138.3, 135.6, 134.4, 132.1, 123.4, 58.6, 46.0, 38.9, 34.0, 32.00, 31.8, 29.5, 29.4, 29.3, 29.2, 29.0, 25.2, 24.6, 22.6, 20.1, 14.4.

*4.2.8. 2-(3-hydroxy-1,1-dimethylpropyl)-3,5-dimethylphenyl myristate **3e***

Starting from 3.00 g (9.30 mmol) of phenol **1** and 2.55 g (11.2 mmol) of myristic acid, 2.90 g (6.93 mmol, 74%) of alcohol **3e** was obtained as colourless oil.

^{1}H NMR (500 MHz, DMSO-d_6) δ: 6.36 (s, 1H), 6.23 (s, 1H), 3.73 (br, 1H), 3.22 (m, 2H), 2.29 (t, 2H, J = 7.4 Hz), 2.11 (s, 3H), 2.04 (s, 3H), 2.00 (m, 2H), 1.38 (quint, 2H, J = 7.1 Hz), 1.40 (s, 6H), 1.25–1.10 Hz (br, 20H), 0.76 (t, 3H, J = 7.4 Hz). ^{13}C NMR (125 MHz, DMSO-d_6) δ: 173.1, 156.7, 136.9, 135.1, 127.4, 125.6, 115.8, 62.7, 33.7, 31.7, 31.6, 29.3, 29.3, 29.2, 29.1, 29.0, 28.9, 28.7, 25.5, 24.6, 22.4, 20.3, 14.2.

*4.2.9. 2-(3-hydroxy-1,1-dimethylpropyl)-3,5-dimethylphenyl palmitate **3f***

Starting from 2.00 g (6.20 mmol) of phenol **1** and 1.91 g (7.40 mmol) of palmitic acid, 1.54 g (3.45 mmol, 56%) of alcohol **3f** was obtained as a white solid. ^{1}H NMR (500 MHz, DMSO-d_6) δ: 6.45 (s, 1H), 6.32 (s, 1H), 3.81 (t, 2H, J = 7.4 Hz), 2.37 (s, 3H), 2.20 (t, 2H, J = 7.4 Hz), 2.13 (t, 2H, J = 7.4 Hz), 2.09 (s, 3H), 1.47 (s, 6H), 1.43 (m, 2H), 1.38 (s, 1H), 1.31–1.12 (br, 24H), 0.85 (t, 3H, J = 6.8 Hz). ^{13}C NMR (125 MHz, DMSO-d_6) δ: 173.3, 156.9, 137.1, 135.3, 127.6, 125.8, 116.0, 62.9, 33.9, 31.9, 31.8, 29.5, 29.5, 29.4, 29.32, 29.2, 29.1, 28.8, 25.7, 24.8, 22.6, 20.5, 14.4.

*4.2.10. 2-(3-hydroxy-1,1-dimethylpropyl)-3,5-dimethylphenyl stearate **3g***

Starting from 3.30 g (10.3 mmol) of phenol **1** and 3.49 g (12.3 mmol) of stearic acid, 1.54 g (2.86 mmol, 59%) of alcohol **3g** was obtained as a white solid. ^{1}H NMR (500 MHz, DMSO-d_6) δ: 6.82 (s, 1H), 6.54 (s, 1H), 4.24 (t, 1H, J = 6.0 Hz), 3.21 (m, 2H), 2.53 (t, 2H, J = 7.5 Hz), 2.47 (s, 3H), 2.17 (s, 3H), 1.90 (m, 2H), 1.62 (quint, 2H, J = 7.3 Hz), 1.39 (s, 6H), 1.37–1.19 (br, 28H) 0.86 (t, 3H, 7.5 Hz). ^{13}C NMR (125 MHz, DMSO-d_6) δ: 172.6, 150.0, 138.3, 135.7, 134.4, 132.1, 123.6, 58.7, 46.0, 39.0, 34.6, 32.0, 31.8, 29.5, 29.5, 29.4, 29.3, 29.2, 29.1, 28.9, 25.5, 24.6, 22.6, 20.1, 14.4.

*4.2.11. 2-(2-oxo-1,1-dimethylethyl}-O-acyloyl-3,5-dimethylphenol (**4a-g**) – general procedure*

The reaction was carried out under argon atmosphere. To a stirred solution of 7.74 mmol. of alcohol **3** dissolved in dry DCM, 15 mmol of PCC was added in one portion. The reaction mixture was stirred at room temperature for 4 h and then was filtered through silica gel using a mixture of hexane/AcOEt, 8/2, v/v as an eluent.

*4.2.12. 2-(2-oxo-1,1-dimethylethyl)-3,5-dimethylphenyl acetate **4a***

Starting from 1.50 g (5.99 mmol) of alcohol **3a**, 1.30 g (5.24 mmol, 87%) of aldehyde **4a** was obtained as a light-yellow oil.

^{1}H NMR (500 MHz, DMSO-d_6) δ: 9.47 (t, 1H, J = 2.3 Hz), 6.88 (s, 1H), 6.64 (s, 1H), 2.82 (d, 2H, J = 2.3 Hz), 2.49 (s, 3H), 2.31 (s, 3H), 2.27 (s, 3H), 2.18 (s, 3H), 1.49 (s, 6H). ^{13}C NMR (125 MHz, DMSO-d_6) δ: 203.1, 170.2, 149.6, 138.0, 136.4, 133.4, 132.5, 123.8, 56.4, 38.1, 31.5, 25.3, 22.0, 20.12.

*4.2.13. 2-(2-oxo-1,1-dimethylethyl)-3,5-dimethylphenyl caprylate **4b***

Starting from 2.50 g (7.74 mmol) of alcohol **3b**, 1.85 g (5.56 mmol, 74%) of aldehyde **4b** was obtained as a light-yellow oil.

^{1}H NMR (500 MHz, DMSO-d_6) δ: 9.46 (t, 1H, J = 2.3 Hz), 6.85 (s, 1H), 6.60 (s, 1H), 2.81 (d, 2H, J = 2.2 Hz), 2.57 (t, 2H, J = 7.5 Hz), 2.50 (s, 3H), 2.18 (s, 3H), 1.63 (quint, 2H, J = 7.0 Hz), 1.48 (s, 6H), 1.39–1.22 (br, 8H), 0.88 (t, 3H, J = 7.6 Hz). ^{13}C NMR (125 MHz, DMSO-d_6) δ: 202.9, 172.6, 149.7, 138.0, 136.4, 133.4, 132.4, 123.7, 56.4, 38.1, 34.6, 31.8, 31.5, 29.3, 29.2, 29.1, 28.9, 25.3, 24.6, 22.6, 20.1.

*4.2.14. 2-(2-oxo-1,1-dimethylethyl)-3,5-dimethylphenyl caprate **4c***

Starting from 1.20 g (3.31 mmol) of alcohol **3c**, 1.08 g (3.00 mmol, 91%) of aldehyde **4c** was obtained as light-yellow oil.

^{1}H NMR (500 MHz, DMSO-d_6) δ: 9.47 (t, 1H, J = 2.4 Hz), 6.85 (s, 1H), 6.60 (s, 1H), 2.81 (d, 2H, J = 2.4 Hz), 2.56 (t, 2H, J = 7.5 Hz), 2.50 (s, 3H), 2.18 (s, 3H), 1.47 (s, 6H), 1.63 (quint, 2H, J = 7.0 Hz), 1.40–1.19 (br, 12H), 0.87 (t, 3H, J = 7.5 Hz). ^{13}C NMR (125 MHz, DMSO-d_6) δ: 202.7, 172.5, 149.5, 137.8, 136.2, 133.2, 132.2, 123.5, 56.2, 37.9, 34.4, 31.6, 31.4, 29.2, 29.0, 29.0, 28.7, 25.1, 24.4, 22.4, 20.0, 14.2.

*4.2.15. 2-(2-oxo-1,1-dimethylethyl)-3,5-dimethylphenyl laurate **4d***

Starting from 1.67 g (4.28 mmol) of alcohol **3d**, 1.25 g (3.22 mmol, 75%) of aldehyde **4d** was obtained as a light-yellow oil.

^{1}H NMR (500 MHz, DMSO-d_6) δ: 9.46 (t, 1H, J = 2.2 Hz), 6.85 (s, 1H), 6.59 (s, 1H), 2.80 (d, 2H, J = 2.3 Hz), 2.56 (t, 2H, J = 7.3 Hz), 2.49 (s, 3H), 2.18 (s, 3H), 1.63 (quint, 2H, J = 7.2 Hz), 1.47 (s, 6H), 1.39–1.20 (br, 16H), 0.86 (t, 3H, J = 7.4 Hz). ^{13}C NMR (125 MHz, DMSO-d_6) δ: 203.0, 172.7, 149.7, 138.0, 136.4, 133.4, 132.4, 123.7, 56.4, 38.1, 34.5, 31.8, 31.5, 31.2, 29.5, 29.5, 29.3, 29.2, 29.1, 28.9, 25.3, 24.5, 22.6, 20.1, 14.4.

*4.2.16. 2-(2-oxo-1,1-dimethylethyl)-3,5-dimethylphenyl myristate **4e***

Starting from 2.00 g (4.78 mmol) of alcohol **3e**, 1.45 g (3.48 mmol, 73%) of aldehyde **4e** was obtained as a light-yellow oil.

^{1}H NMR (500 MHz, DMSO-d_6) δ: 9.42 (m, 1H), 6.82 (s, 1H), 6.55 (s, 1H), 2.77 (s, 2H), 2.53 (t, 2H, J = 7.2 Hz), 2.46 (s, 3H), 2.14 (s, 3H), 1.59 (quint, 2H, J = 7.2 Hz), 1.44 (s, 6H), 1.35–1.18 (br, 20H), 0.82 (t, 3H, J = 7.1 Hz). ^{13}C NMR (125 MHz, DMSO-d_6) δ: 203.2, 172.9, 149.8, 138.2, 136.5, 133.5, 132.6, 123.8, 56.6, 38.3, 34.7, 31.9, 31.7, 29.7, 29.6, 29.6, 29.4, 29.3, 29.3, 29.0, 25.5, 24.7, 22.7, 20.3, 14.6.

*4.2.17. 2-(2-oxo-1,1-dimethylethyl)-3,5-dimethylphenyl palmitate **4f***

Starting from 1.19 g (2.66 mmol) of alcohol **3f**, 940 mg (2.12 mmol, 79%) of aldehyde **4f** was obtained as a light-yellow oil.

^{1}H NMR (500 MHz, DMSO-d_6) δ: 9.46 (m, 1H), 6.85 (s, 1H), 6.59 (s, 1H), 2.80 (s, 2H), 2.57 (t, 2H, J = 7.4 Hz), 2.50 (s, 3H), 2.18 (s, 3H), 1.63 (quint, 2H, J = 7.2 Hz), 1.48 (s, 6H), 1.37–1.20 (br, 24H), 0.86 (t, 3H, J = 7.4 Hz). ^{13}C NMR (125 MHz, DMSO-d_6) δ: 203.1, 172.7, 149.7, 138.0, 136.4, 133.4, 132.4, 123.7, 56.4, 38.1, 34.5, 31.8, 31.5, 29.5, 29.5, 29.4, 29.3, 29.2, 29.10, 28.9, 25.3, 24.5, 22.6, 20.2, 14.4.

*4.2.18. 2-(2-oxo-1,1-dimethylethyl)-3,5-dimethylphenyl stearate **4g***

Starting from 2.90 g (6.11 mmol) of alcohol **3g**, 2.50 g (5.29 mmol, 87%) of aldehyde **4g** was obtained as a light-yellow waxy solid.

^{1}H NMR (500 MHz, DMSO-d_6): 9.46 (m, 1H), 6.85 (s, 1H), 6.59 (s, 1H), 2.80 (s, 2H), 2.56 (t, 2H, J = 7.7 Hz), 2.49 (s, 3H), 2.18 (s, 3H), 1.63 (quint, 2H, J = 7.2 Hz), 1.48 (s, 6H), 1.42–1.19 (br, 28H), 0.86 (t, 3H, J = 7.3 Hz). ^{13}C NMR (125 MHz, DMSO-d_6) δ: 203.0, 172.7, 149.7, 138.0, 136.4, 133.4, 132.4, 123.7, 38.1, 35.0, 34.5, 31.8, 31.5, 31.3, 29.76, 29.5, 29.4, 29.3, 29.2, 29.1, 28.9, 25.3, 24.5, 22.6, 20.1, 14.4.

2-(3-hydroxycarbonyl-1,1-dimethylethyl}-*O*-acyloyl-3,5-dimethylphenol (**5a-g**) – general procedure 5.86 mmol of aldehyde **4** was dissolved in 100 mL of the mixture of acetone/*tert*BuOH/H_2O (6/4/1, v/v/v) and then 7.06 mmol of NaH_2PO_4, 2 mL of 2-methylbut-2-ene and 28.2 mmol of $NaClO_2$ were added respectively. The mixture was allowed to stir for 18 h at room temperature and then poured onto 500 mL of saturated solution of $NH_4Cl_{(aq)}$. The mixture was extracted with diethyl ether and the organic layer was washed with water. Organic layer was

dried under anhydrous $MgSO_4$, the desiccant was filtered off ant the filtrate was concentrated under reduced pressure.

4.2.19. 2-(2-hydroxycarbonyl-1,1-dimethylethyl)-3,5-dimethylphenyl acetate **5a**

Starting from 1.10 g (4.43 mmol) of aldehyde **4a**, 1.05 g (3.97 mmol, 90%) of carboxylic acid **5a** was obtained as white solid.

^{1}H NMR (500 MHz, DMSO-d_6) δ: 11.85 (s, 1H), 6.80 (s, 1H), 6.60 (s, 1H), 2.71 (s, 2H), 2.49 (s, 3H), 2.26 (s, 3H), 2.17 (s, 3H), 1.47 (s, 6H). ^{13}C NMR (125 MHz, DMSO-d_6) δ: 173.1, 170.0, 149.7, 138.1, 135.6, 134.3, 132.1, 123.5, 79.6, 47.9, 38.6, 31.4, 25.3, 22.0, 20.1.

4.2.20. 2-(2-hydroxycarbonyl-1,1-dimethylethyl)-3,5-dimethylphenyl caprylate **5b**

Starting from 1.65 g (4.96 mmol) of aldehyde **4b**, 1.58 g (4.53 mmol, 91%) of carboxylic acid **5b** was obtained as white solid.

^{1}H NMR (500 MHz, DMSO-d_6) δ: 11.82 (br, 1H), 6.80 (s, 1H), 6.56 (s, 1H), 2.70 (s, 2H), 2.56 (t, 2H, $J = 7.2$ Hz), 2.50 (s, 3H), 2.17 (s, 3H), 1.63 (m, 2H), 1.47 (s, 6H), 1.38–1.22 (br, 8H), 0.88 (t, 3H, $J = 7.2$ Hz). ^{13}C NMR (125 MHz, DMSO-d_6) δ: 173.1, 172.6, 149.9, 138.2, 135.7, 134.4, 132.1, 123.5, 47.9, 38.8, 34.7, 31.8, 31.5, 29.2, 29.0 25.4, 24.6, 22.7, 20.2, 14.5.

4.2.21. 2-(2-hydroxycarbonyl-1,1-dimethylethyl)-3,5-dimethylphenyl caprate **5c**

Starting from 880 mg (2.44 mmol) of aldehyde **4c**, 850 mg (2.26 mmol, 92%) of carboxylic acid **5c** was obtained as a white solid.

^{1}H NMR (500 MHz, DMSO-d_6) δ: 11.82 (br, 1H), 6.80 (s, 1H), 6.56 (s, 1H), 2.70 (s, 2H), 2.56 (t, 2H, $J = 7.1$ Hz), 2.50 (s, 3H), 2.17 (s, 3H), 1.64 (m, 2H), 1.47 (6H), 1.39–1.21 (br, 12H), 0.87 (t, 3H, $J = 7.1$ Hz). ^{13}C NMR (125 MHz, DMSO-d_6) δ: 173.0, 172.5, 138.1, 135.6, 134.4, 132.1, 123.4, 47.8, 38.7, 34.6, 31.8, 31.5, 31.4, 29.3, 29.2, 29.1, 28.9, 25.3, 24.6, 22.6, 20.1, 14.4.

4.2.22. 2-(2-hydroxycarbonyl-1,1-dimethylethyl)-3,5-dimethylphenyl laurate **5d**

Starting from 1.2 g (3.09 mmol) of aldehyde **4d**, 1.15 g (2.84 mmol, 92%) of carboxylic acid **5d** was obtained as a white solid.

^{1}H NMR (500 MHz, DMSO-d_6) δ: 11.82 (br, 1H), 6.80 (s, 1H), 6.56 (s, 1H), 2.70 (s, 2H), 2.56 (t, 2H, $J = 7.2$ Hz), 2.50 (s, 3H), 2.17 (s, 3H), 1.63 (m, 2H), 1.46 (s, 6H), 1.39–1.25 (br, 16H), 0.87 (t, 3H, $J = 7.2$ Hz). ^{13}C NMR (125 MHz, DMSO-d_6) δ: 173.1, 172.6, 149.8, 138.1, 135.6, 134.4, 132.1, 123.4, 47.9, 38.7, 34.6, 31.8, 31.4, 29.5, 29.34, 29.2, 29.1, 28.9, 25.3, 24.5, 22.6, 20.1, 14.4.

4.2.23. 2-(2-hydroxycarbonyl-1,1-dimethylethyl)-3,5-dimethylphenyl myristate **5e**

Starting from 1.40 g (3.36 mmol) of aldehyde **4e**, 1.40 g (3.24 mmol, 96%) of carboxylic acid **5e** was obtained as a white solid.

^{1}H NMR (500 MHz, DMSO-d_6) δ: 11.84 (br, 1H), 6.80 (s, 1H), 6.55 (s, 1H), 2.70 (s, 2H), 2.56 (t, 2H, $J = 7.2$ Hz), 2.49 (s, 3H), 2.17 (s, 3H), 1.63 (m, 2H), 1.46 (s, 6H), 1.35–1.19 (br, 20H), 0.87 (t, 3H, $J = 7.3$ Hz). ^{13}C NMR (125 MHz, DMSO-d_6) δ: 173.04, 172.6, 149.8, 138.1, 135.6, 134.3, 132.1, 123.4, 71.8, 67.2, 47.8, 38.7, 34.6, 31.8, 31.4, 29.5, 29.5, 29.4, 29.3, 29.2, 29.1, 28.9, 27.3, 25.3, 25.1, 24.6, 22.6, 20.2, 20.1, 14.4.

4.2.24. 2-(2-hydroxycarbonyl-1,1-dimethylethyl)-3,5-dimethylphenyl palmitate **5f**

Starting from 889 mg (2.00 mmol) of aldehyde **4f**, 880 mg (1.91 mmol, 96%) of carboxylic acid **5f** was obtained as a white solid. ^{1}H NMR (500 MHz, DMSO-d_6) δ: 11.84 (s, 1H), 6.80 (s, 1H), 6.55 (s, 1H), 2.70 (s, 2H), 2.56 (t, 2H, $J = 7.2$ Hz), 2.49 (s, 3H), 2.17 (s, 3H), 1.63 (m, 2H), 1.46 (s, 6H), 1.34–1.18 (br, 24H), 0.86 (t, 3H, $J = 7.2$ Hz). ^{13}C NMR (125 MHz, DMSO-d_6) δ: 173.0, 172.5, 149.8, 138.1, 135.6, 134.3, 132.1, 123.4, 47.8, 38.7, 34.6, 31.8, 31.4, 29.6, 29.5, 29.5, 29.4, 29.3, 29.2, 29.1, 28.9, 25.3, 24.6, 22.6, 20.2, 14.4.

4.2.25. 2-(2-hydroxycarbonyl-1,1-dimethylethyl)-3,5-dimethylphenyl stearate **5g**

Starting from 2.5 g (5.29 mmol) of aldehyde **4g**, 2.28 mg (4.67 mmol, 88%) of carboxylic acid **6g** was obtained as a white solid.

^{1}H NMR (500 MHz, DMSO-d_6) δ: 11.8 (br, 1H), 6.77 (s, 1H), 6.53 (s, 1H), 2.67 (s, 2H), 2.53 (t, 2H, $J = 6.9$ Hz), 2.47 (s, 3H), 2.14 (s, 3H), 1.62 (m, 2H), 1.44 (s, 6H), 1.39–1.17 (br, 28H), 0.83 (t, 3H, $J = 7.2$ Hz). ^{13}C NMR (125 MHz, DMSO-d_6) δ: 173.0, 172.5, 149.8, 138.1, 135.6, 134.32, 132.1, 123.4, 47.8, 38.7, 34.6, 31.8, 31.4, 29.5, 29.5, 29.4, 29.3, 29.2, 29.1, 28.90, 25.3, 24.6, 22.6, 20.1, 14.44.

4.2.26. 2-(3-hydroxycarbonyl-1,1-dimethylethyl}-O-acyloyl-3,5-dimethylphenol/5-fluorocytosine conjugate (**6a-g**) – general procedure

A solution of 1.43 mmol of a carboxylic acid **5** and 0.2 mmol of anhydrous DMF in 5 mL of anhydrous DCM was cooled to 0 °C and then 2.14 mmol of oxalyl chloride was added dropwise. The mixture was stirred at 0 °C for 30 min and then for additional 2 h at room temperature. The mixture was concentrated under reduced pressure (max. bath temperature of 30 °C) and the residue was dissolved in 5 mL of anhydrous DCM. The prepared chloride was added dropwise to a suspension made of 5-fluorocytosine (1.35 mmol), DMAP (0.27 mmol), and pyridine (2.03 mmol) in 2 mL of anhydrous DCM at 0 °C. The mixture was stirred at 0 °C for 30 min, and then at room temperature for additional 2 h. The resulting mixture was diluted with 10 mL of DCM and washed with 0.5 M $HCl_{(aq)}$ and brine, respectively. The organic layer was dried over anhydrous $MgSO_4$, the desiccant was filtered off and the filtrate was concentrated *in vacuo*. The residue was purified by flash chromatography on silica gel, using chloroform (A) and a mixture of solvents $CHCl_3$/MeOH/H_2O (130/10/1, v/v/v) (B) (0% B → 100% B) as a mobile phase.

4.2.27. 2-(2-hydroxycarbonyl-1,1-dimethylethyl)-3,5-dimethylphenyl acetate/5-fluorocytosine conjugate **6a**

Starting from 200 mg (0.76 mmol) of carboxylic acid **5a**, 120 mg (0.32 mmol, 42%) of conjugate **6a** was obtained as a yellow-brown solid.

^{1}H NMR (500 MHz, $CDCl_3$ + TFA) δ 8.12 (m, 1H, H17), 6.79 (s, 1H, H4), 6.59 (s, 1H, H2), 3.04 (s, 2H, H11), 2.51 (s, 3H, H19), 2.26 (s, 3H, H8), 2.16 (s, 3H, H7), 1.49 (s, 6H, H18). ^{13}C signals from ^{1}H – ^{13}C HSQC and HMBC experiments ($CDCl_3$ + TFA) δ: 175.2 (C12), 173.2 (C18), 151.2 (C13), 149.7 (C1), 144.3 (C14), 138.9 (C17), 133.5 (C4), 133.1 (C16), 131.5 (C6), 131.0 (C3), 123.6 (C2), 123.5 (C5), 50.7 (C9), 40.2 (C11), 31.5 (C10), 25.2 (C7), 19.9 (C19), 19.8 (C8).

4.2.28. 2-(2-hydroxycarbonyl-1,1-dimethylethyl)-3,5-dimethylphenyl caprylate/5-fluorocytosine conjugate **6b**

Starting from 500 mg (1.43 mmol) of carboxylic acid **5b**, 352 mg (0.77 mmol, 53%) of conjugate **6b** was obtained as a yellow-brown solid.

^{1}H NMR (500 MHz, DMSO-d_6 + TFA) δ: 8.22 (d, 1H, $J = 5.1$ Hz, H17), 6.78 (s, 1H. H4), 6.53 (s, 1H, H2), 3.07 (s, 2H, H11), 2.56 (t, 2H, $J = 7.4$ Hz, H19), 2.51 (s, 3H, H8), 2.16 (s, 3H, H7), 1.60 (m, 2H, H20), 1.48 (s, 6H, H10), 1.35–1.20 (br, 8H, H22, multiple CH_2 groups, overlapped), 0.86 (m, 3H, H21). ^{13}C signals from ^{1}H – ^{13}C HSQC and HMBC experiments ($CDCl_3$ + TFA) δ: 172.6 (C18), 171.6 (C12), 149.7 (C1), 154.1 (C16), 153.0 (C13), 139.4 (C14), 138.7(C5), 134.6 (C6), 134.4 (C3, C5 overlapped), 132.0 (C4), 131.6 (C17), 123.4 (C2), 49.7 (C11), 38.9 (C9), 34.4 (C19), 31.3 (C10), 25.2 (C8), 24.4 (C20), 22.3 (C22, multiple CH_2 groups, overlapped), 19.9 (C7), 14.2 (C21).

4.2.29. 2-(2-hydroxycarbonyl-1,1-dimethylethyl)-3,5-dimethylphenyl caprate/5-fluorocytosine conjugate **6c**

Starting from 100 mg (0.27 mmol) of carboxylic acid **5c**, 75 mg (0.15 mmol, 68%) of conjugate **6c** was obtained as a light-brown solid.

^{1}H NMR (500 MHz, DMSO-d_6 + TFA) δ 8.18 (d, 1H, $J = 5.1$ Hz, H17), 6.78 (s, 1H. H4), 6.53 (s, 1H, H2), 3.06 (s, 2H, H11), 2.56 (t, 2H, $J = 7.2$

Hz, H19), 2.50 (s, 3H, H8), 2.15 (s, 3H, H7), 1.60 (m, 2H, H20), 1.48 (s, 6H, H10), 1.35–1.20 (br, 12H, H22, multiple CH_2 groups, overlapped), 0.86 (m, 3H, H21). ^{13}C signals from ^1H – ^{13}C HSQC and HMBC experiments ($CDCl_3$ + TFA) δ: 172.6 (C18), 171.6 (C12), 154.1 (C16), 149.7 (C1), 149.7 (C13), 139.2 (C14), 138.0 (C5), 134.4 (C6), 134.3 (C3, C5 overlapped), 132.1 (C4), 132.1 (C17), 123.4 (C2), 49.9 (C11), 39.6 (C9), 34.4 (C19), 31.3 (C10), 25.2 (C8), 24.6 (C20), 22.5 (C22, multiple CH_2 groups, overlapped), 19.9 (C7), 14.1 (C21).

4.2.30. 2-(2-hydroxycarbonyl-1,1-dimethylethyl)-3,5-dimethylphenyl laurate/5-fluorocytosine conjugate **6d**

Starting from 200 mg (0.49 mmol) of carboxylic acid **6d**, 122 mg (0.23 mmol, 47%) of conjugate **6d** was obtained as a yellowish solid.

^1H NMR (500 MHz, $CDCl_3$ + TFA) δ 7.97 (d, 1H, J = 4.5 Hz, H17), 6.81 (s, 1H, H4), 6.58 (s, 1H, H2), 3.03 (s, 2H, H11), 2.60 (t, 2H, J = 7.2 Hz, H19), 2.52 (s, 3H, H8), 2.23 (s, 3H, H7), 1.76 (m, 2H, H20), 1.65 (s, 6H, H10), 1.36–1.20 (br, 16H, H22, multiple CH_2 groups, overlapped), 0.89 (t, 3H, J = 6.9 Hz, H21). ^{13}C signals from ^1H – ^{13}C HSQC and HMBC experiments ($CDCl_3$ + TFA) δ: 175.2 (C18), 174.1 (C12), 156.2 (C13), 153.2 (C16), 149.8 (C1), 138.4 (C3) 138.2 (C14), 136.8 (C5), 136.2 (C6), 132.9 (C17), 132.7 (C4), 123.4 (C2), 49.9 (C11), 39.6 (C9), 35.0 (C19), 31.6 (C10), 29.6(C22, multiple CH_2 groups, overlapped), 25.4 (C8), 24.6 (C20), 19.9 (C7), 14.0 (C21).

4.2.31. 2-(2-hydroxycarbonyl-1,1-dimethylethyl)-3,5-dimethylphenyl myristate/5-fluorocytosine conjugate **6e**

Starting from 300 mg (0.69 mmol) of carboxylic acid **5e**, 160 mg (0.29 mmol, 42%) of conjugate **6e** was obtained as a yellow-brown solid.

^1H NMR (500 MHz, $CDCl_3$ + TFA) δ 7.97 (d, 1H, J = 4.1 Hz, H17), 6.89 (s, 1H, H4), 6.60 (s, 1H, H2), 2.90 (s, 2H, H11), 2.68 (t, 2H, J = 6.9 Hz, H19), 2.50 (s, 3H, H8), 2.25 (s, 3H, H7), 1.80 (m, 2H, H20), 1.71 (s, 6H, H10), 1.35–1.19 (br, 20H, H22, multiple CH_2 groups, overlapped), 0.90 (t, 3H, J = 7.0 Hz, H21).). ^{13}C signals from ^1H – ^{13}C HSQC and HMBC experiments ($CDCl_3$ + TFA) δ: 177.7 (C18), 175.2 (C12), 153.2 (C16), 151.0 (C13), 150.4 (C1), 138.4 (C3) 138.2 (C14), 136.8 (C5), 134.0 (C6), 133.6 (C4), 132.9 (C17), 123.6 (C2), 50.6 (C11), 39.6 (C9), 35.0 (C19), 31.6 (C10), 29.6 (C22, multiple CH_2 groups, overlapped), 25.4 (C8), 24.5 (C20), 19.9 (C7), 14.0 (C21).

4.2.32. 2-(2-hydroxycarbonyl-1,1-dimethylethyl)-3,5-dimethylphenyl palmitate/5-fluorocytosine conjugate **6f**

Starting from 100 mg (0.22 mmol) of carboxylic acid **5f**, 63 mg (0.11 mmol, 51%) of conjugate **6f** was obtained as a light-brown solid.

^1H NMR (500 MHz, DMSO-d_6 + TFA) δ 8.39 (d, 1H, J = 4.5 Hz, H17), 6.75 (s, 1H. H4), 6.50 (s, 1H, H2), 3.13 (s, 2H, H11), 2.52 (m, 2H, H19), 2.48 (s, 3H, H8), 2.12 (s, 3H, H7), 1.59 (m, 2H, H20), 1.49 (s, 6H, H10), 1.29–1.11 (br, 24H, H22, multiple CH_2 groups, overlapped), 0.80 (m, 3H, H21). ^{13}C signals from ^1H – ^{13}C HSQC and HMBC experiments (DMSO-d_6 + TFA) δ: 172.5 (C18), 171.7 (C12), 149.7 (C1), 152.4 (C16), 149.7 (C13), 138.0 (C14), 136.4 (C5), 134.5 (C6), 134.3 (C3), 131.9 (C4), 132.1 (C17), 123.2 (C2), 50.2 (C11), 39.2 (C9), 35.4 (C19), 30.9 (C10), 25.0 (C8), 24.6 (C20), 22.5 (C22, multiple CH_2 groups, overlapped), 19.5 (C7), 13.7 (C21).

4.2.33. 2-(2-hydroxycarbonyl-1,1-dimethylethyl)-3,5-dimethylphenyl stearate/5-fluorocytosine conjugate **6g**

Starting from 500 mg (1.02 mmol) of carboxylic acid **5g**, 223 mg (0.37 mmol, 36%) of conjugate **6g** was obtained as a light-brown solid.

^1H NMR (500 MHz, DMSO-d_6 + TFA) δ 8.10 (s, 1H, H17), 6.78 (s, 1H, H4), 6.53 (s, 1H, H2), 3.03 (s, 2H, H11), 2.52 (m, 2H, H19), 2.48 (s, 3H, H8), 2.12 (s, 3H, H7), 1.60 (m, 2H, H20), 1.48 (s, 6H, H10), 1.41–1.15 (br, 28H, H22, multiple CH_2 groups, overlapped), 0.85 (m, 3H, H21). ^{13}C signals from ^1H – ^{13}C HSQC and HMBC experiments (DMSO-d_6 + TFA) δ: 172.6 (C18), 171.6 (C12), 149.7 (C1), 155.0 (C16), 149.7 (C13), 138.0 (C14), 136.4 (C5), 134.5 (C6), 134.3 (C3), 131.9 (C4), 132.0 (C17), 123.3 (C2), 49.7 (C11), 40.0 (C9), 34.4 (C19), 29.3 (C10), 25.3 (C8), 24.4 (C20), 22.1 (C22, multiple CH_2 groups, overlapped), 20.0 (C7), 14.2 (C21).

4.2.34. 2-(3-hydroxycarbonyl-1,1-dimethylethyl}-O-acyloyl-3,5-dimethylphenol active ester (**7a-g**) – general procedure

To the solution of 1.43 mmol of a carboxylic acid **5** in anhydrous DMF, 2.9 mmol of DEPBT and 1 mL of DIPEA were added. The mixture was allowed to stir at room temperature for 5 h 30 mL of chloroform was added and the formed layers were separated. The organic layer was washed with 1 M $HCl_{(aq)}$, brine, saturated $NaHCO_{3(aq)}$ and brine, respectively. The organic layer was dried under anhydrous $MgSO_4$, the desiccant was filtered off and the filtrate was concentrated *in vacuo*. The residue was purified by flash chromatography on silica gel, using a mixture of solvents hexanes/AcOEt (0% → 50%) as a mobile phase.

4.2.35. 2-(2-hydroxycarbonyl-1,1-dimethylethyl)-3,5-dimethylphenyl acetate active ester **7a**

Starting from 500 mg (1.89 mmol) of carboxylic acid **5a**, 180 mg (1.18 mmol, 62%) of active ester **7a** was obtained as a colourless oil and used for further synthesis without spectral characterisation. R_f 0.61 (hexanes/AcOEt, 5/5, v/v).

4.2.36. Syntheses2-(2-hydroxycarbonyl-1,1-dimethylethyl)-3,5-dimethylphenyl caprylate active ester **7b**

Starting from 500 mg (1.43 mmol) of carboxylic acid **5b**, 560 mg (1.13 mmol, 79%) of active ester **7b** was obtained as a colourless oil and used for further synthesis without spectral characterisation. R_f 0.61 (hexanes/AcOEt, 7/3, v/v).

4.2.37. 2-(2-hydroxycarbonyl-1,1-dimethylethyl)-3,5-dimethylphenyl caprate active ester **7c**

Starting from 660 mg (1.75 mmol) of carboxylic acid **5c**, 610 mg (1.17 mmol, 67%) of active ester **7c** was obtained as a colourless solid and used for further synthesis without spectral characterisation. R_f 0.68 (hexanes/AcOEt, 7/3, v/v).

4.2.38. 2-(2-hydroxycarbonyl-1,1-dimethylethyl)-3,5-dimethylphenyl laurate active ester **7d**

Starting from 800 mg (1.98 mmol) of carboxylic acid **5d**, 720 mg (1.31 mmol, 66%) of active ester **7d** was obtained as a colourless solid and used for further synthesis without spectral characterisation. R_f 0.72 (hexanes/AcOEt, 7/3, v/v).

4.2.39. 2-(2-hydroxycarbonyl-1,1-dimethylethyl)-3,5-dimethylphenyl myristate active ester **7e**

Starting from 900 mg (2.08 mmol) of carboxylic acid **5e**, 890 mg (1.54 mmol, 74%) of active ester **7e** was obtained as a colourless oil and used for further synthesis without spectral characterisation. R_f 0.76 (hexanes/AcOEt, 7/3, v/v).

4.2.40. 2-(2-hydroxycarbonyl-1,1-dimethylethyl)-3,5-dimethylphenyl palmitate active ester **7f**

Starting from 750 mg (1.63 mmol) of carboxylic acid **5f**, 780 mg (1.29 mmol, 79%) of active ester **7f** was obtained as a colourless solid and used for further synthesis without spectral characterisation. R_f 0.43 (hexanes/AcOEt, 8/2, v/v).

4.2.41. 2-(2-hydroxycarbonyl-1,1-dimethylethyl)-3,5-dimethylphenyl stearate active ester **7g**

Starting from 1.1 g (2.25 mmol) of carboxylic acid **5g**, 1.07 g (1.69 mmol, 75%) of active ester **7g** was obtained as colourless solid and used for further synthesis without spectral characterisation. R_f 0.59 (hexanes/AcOEt, 8/2, v/v).

*4.2.42. 2-(3-hydroxycarbonyl-1,1-dimethylethyl}-O-acyloyl-3,5-dimethylphenol/Nap-NH_2 conjugate (**8a-g**) – general procedure*

0.30 mmol of an active ester **7** was dissolved in 10 mL of anhydrous DMF and then 0.32 mmol of Nap-NH_2 and 1 mmol of DIPEA were added. The mixture was stirred at room temperature for 4 h. Subsequently, the mixture was poured onto 50 mL of saturated $NaHCO_{3(aq)}$ and extracted with AcOEt. The organic layer washed with saturated $NaHCO_{3(aq)}$, and then dried over anhydrous $MgSO_4$. The desiccant was filtered off and the filtrate was concentrated under reduced pressure. The residue was purified by flash chromatography on silica gel, using a mixture of solvents hexanes/AcOEt (0% → 100%) as a mobile phase.

*4.2.43. 2-(2-hydroxycarbonyl-1,1-dimethylethyl)-3,5-dimethylphenyl acetate/Nap-NH_2 conjugate **8a***

Starting from 200 mg (0.49 mmol) of active ester **7a**, 230 mg (0.32 mmol, 87%) of product **8**was obtained as a yellow solid.

^{1}H NMR (500 MHz, $CDCl_3$) δ: 8.61 (s, 1H, J = 7.3Hz), 8.46 (d, 1H, J = 7.6 Hz), 8.27 (d, 1H, J = 8.3 Hz), 7.66 (t, 1H, J = 7.9 Hz), 6.56 (s, 1H), 6.54 (s, 1H), 6.45 (s, 1H, J = 8.5 Hz), 6.19 (t, 1H, J = 6.2 Hz), 4.29 (m, 1H), 4.19 (m, 2H), 3.49 (m, 2H), 3.10 (m, 2H), 2.32 (s, 3H), 2.19 (s, 3H), 2.11 (s, 3H), 1.74 (m, 2H), 1.62 (s, 6H), 1.46 (m, 4H), 0.99 (t, 3H, J = 7.2 Hz). ^{13}C NMR (125 MHz, $CDCl_3$) δ: 174.3, 172.0, 166.0, 164.9, 164.3, 150.0, 149.9, 138.8, 137.1, 134.5, 132.9, 132.4, 131.1, 129.8, 129.5, 127.3, 124.7, 123.4, 122.8, 120.3, 109.8, 103.1, 67.8, 49.9, 46.5, 40.3, 40.0, 38.9, 38.5, 30.6, 30.4, 29.0, 25.3, 24.0, 23.0, 22.0, 20.5, 20.1, 14.0, 13.9, 11.1.

*4.2.44. 2-(2-hydroxycarbonyl-1,1-dimethylethyl)-3,5-dimethylphenyl caprylate/Nap-NH_2 conjugate **8b***

Starting from 150 mg (0.3 mmol) of active ester **7b**, 185 mg (0.29 mmol, 95%) of product **8b** was obtained as a yellow solid.

^{1}H NMR (500 MHz, $CDCl_3$) δ: 8.59 (s, 1H, J = 7.2Hz), 8.44 (d, 1H, J = 7.7 Hz), 8.25 (d, 1H, J = 8.4 Hz), 7.65 (t, 1H, J = 7.8 Hz), 6.54 (s, 1H), 6.50 (s, 1H), 6.45 (s, 1H, J = 8.4 Hz), 6.28 (t, 1H, J = 6.2 Hz), 4.19 (m, 2H), 3.47 (m, 2H), 3.09 (m, 2H), 2.57 (t, 2H, J = 7.4 Hz), 2.53 (s, 3H), 2.18 (s, 3H), 2.09 (s, 3H), 1.74 (m, 2H), 1.64 (s, 6H), 1.44 (m, 4H), 1.40–1.21 (br, 8H), 0.99 (t, 3H, J = 7.2 Hz) 0.90 (m, 3H). ^{13}C NMR (125 MHz, $CDCl_3$) δ: 175.2, 174.2, 166.0, 164.8, 164.3, 150.2, 150.0, 138.8, 137.1, 134.5, 134.2, 132.7, 132.5, 131.1, 129.8, 129.5,

127.3, 124.7, 123.3, 122.8, 120.4, 109.8, 103.1, 77.0, 76.7, 67.8, 49.9, 46.5, 40.4, 40.0, 38.9, 38.5, 35.1, 32.3, 31.6, 30.6, 30.4, 29.7, 29.1, 29.0, 28.6, 25.3, 24.7, 24.0, 23.0, 22.6, 20.5, 20.1, 14.1, 13.9, 11.1.

*4.2.45. 2-(2-hydroxycarbonyl-1,1-dimethylethyl)-3,5-dimethylphenyl caprate/Nap-NH_2 conjugate **8c***

Starting from 532 mg (1.02 mmol) of active ester **7c**, 630 mg (0.94 mmol, 92%) of product **8c** was obtained as a yellow solid.

^{1}H NMR (500 MHz, $CDCl_3$) δ: 8.61 (s, 1H, J = 7.1Hz), 8.46 (d, 1H, J = 7.5 Hz), 8.27 (d, 1H, J = 8.4 Hz), 7.67 (t, 1H, J = 7.7Hz), 6.56 (s, 1H), 6.52 (s, 1H), 6.47 (s, 1H, J = 8.1 Hz), 6.30 (t, 1H, J = 6.4 Hz), 4.21 (m, 2H), 3.49 (m, 2H), 3.11 (m, 2H), 2.59 (t, 2H, J = 7.1 Hz), 2.55 (s, 3H), 2.18 (s, 3H), 2.11 (s, 3H), 1.76 (m, 2H), 1.64 (s, 6H), 1.464 (m, 4H), 1.39–1.20 (br, 12H), 1.01 (t, 3H, J = 7.2 Hz) 0.92 (m, 3H). ^{13}C NMR (125 MHz, $CDCl_3$) δ: 175.6, 174.7, 165.3, 164.7, 150.6, 150.5, 139.2, 137.5, 134.9, 133.2, 132.9, 131.5, 130.2, 127.7, 125.1, 123.7, 123.2, 120.8, 110.2, 103.5, 77.5, 77.1, 50.3, 46.9, 40.9, 40.4, 39.5, 38.9, 35.6, 32.7, 32.3, 32.3, 30.8, 30.1, 30.0, 29.9, 29.8, 29.6, 29.6, 29.4, 26.4, 25.7, 25.1, 23.1, 20.9, 20.6, 20.5, 14.6, 14.3.

*4.2.46. 2-(2-hydroxycarbonyl-1,1-dimethylethyl)-3,5-dimethylphenyl laurate/Nap-NH_2 conjugate **8d***

Starting from 200 mg (0.36 mmol) of active ester **7d**, 217 mg (0.31 mmol, 85%) of product **8d** was obtained as a yellow solid.

^{1}H NMR (500 MHz, $CDCl_3$) δ: 8.59 (m, 1H), 8.46 (d, 1H, J = 8.4 Hz), 8.27 (d, 1H, J = 8.5 Hz), 7.65 (m, 1H), 7.06 (m, 1H), 6.54 (s, 1H), 6.50 (s, 1H), 6.45 (d, 1H, J = 8.5 Hz), 6.28 (t, 1H, J = 6.2 Hz), 4.19 (m, 2H), 3.48 (m, 2H), 3.09 (d, 2H, J = 4.8 Hz), 2.57 (t, 2H, J = 6.1 Hz), 2.53 (s, 2H), 2.18 (d, 3H), 2.08 (d, 3H J = 9.4 Hz), 1.73 (m, 6H), 1.66 (s, 6H), 1.41–1.16 (br, 16H), 1.00 (t, 7.1 Hz, 3H), 0.90 (t, 8.1 Hz, 3H). ^{13}C NMR (125 MHz, $CDCl_3$) δ: 175.2, 174.2, 166.0, 164.8, 164.3, 150.2, 150.0, 138.8, 137.1, 134.5, 134.2, 132.7, 132.5, 131.1, 129.8, 129.5, 127.3, 124.7, 123.3, 122.8, 120.4, 109.8, 103.1, 77.0, 76.7, 67.8, 49.9, 46.5, 40.4, 40.0, 38.9, 38.5, 35.1, 32.3, 31.6, 30.6, 30.4, 29.7, 29.1, 29.0, 28.6, 25.3, 24.7, 24.0, 23.0, 22.6, 20.5, 20.1, 14.1, 13.9, 11.1.

*4.2.47. 2-(2-hydroxycarbonyl-1,1-dimethylethyl)-3,5-dimethylphenyl myristate/Nap-NH_2 conjugate **8e***

Starting from 210 mg (0.36 mmol) of active ester **7e**, 230 mg (0.32 mmol, 87%) of product **8e** was obtained as a yellow solid.

^{1}H NMR (500 MHz, $CDCl_3$) δ: 8.61 (s, 1H, J = 7.3Hz), 8.45 (d, 1H, J = 7.6 Hz), 8.25 (d, 1H, J = 8.4 Hz), 7.66 (t, 1H, J = 7.7 Hz), 6.56 (s, 1H), 6.54 (s, 1H), 6.46 (s, 1H, J = 8.3 Hz), 6.17 (t, 1H, J = 6.3 Hz), 4.19 (m, 2H), 3.49 (m, 2H), 3.10 (m, 2H), 2.58 (s, 2H), 2.32 (s, 3H), 2.20 (s, 3H), 2.11 (s, 3H), 1.74 (m, 2H), 1.63 (s, 6H), 1.48 (m, 4H), 1.49–1.17 (br, 20H), 0.99 (t, 3H, J = 7.3 Hz), 0.89 (m, 3H). ^{13}C NMR (125 MHz, $CDCl_3$) δ: 175.3, 174.3, 164.9, 164.4, 150.2, 150.1, 138.9, 137.2, 134.6, 132.8, 132.6, 131.2, 129.8, 127.4, 124.8, 123.3, 122.9, 120.4, 109.8, 103.1, 50.0, 46.5, 40.5, 40.0, 38.6, 35.2, 32.3, 32.0, 30.4, 29.8, 29.8, 29.7, 29.7, 29.7, 29.5, 29.4, 29.3, 29.2, 25.4, 24.8, 22.8, 20.5, 20.2, 14.2, 14.0.

*4.2.48. 2-(2-hydroxycarbonyl-1,1-dimethylethyl)-3,5-dimethylphenyl palmitate/Nap-NH_2 conjugate **8f***

Starting from 150 mg (0.25 mmol) of active ester **7f**, 172 mg (0.23 mmol, 90%) of product **8f** was obtained as a yellow solid.

^{1}H NMR (500 MHz, $CDCl_3$) δ: 8.59 (s, 1H, J = 7.4 Hz), 8.45 (d, 1H, J = 7.6 Hz), 8.26 (d, 1H, J = 8.3 Hz), 7.65 (t, 1H, J = 7.6 Hz), 6.54 (s, 1H), 6.50 (s, 1H), 6.44 (s, 1H, J = 8.2 Hz), 6.27 (t, 1H, J = 6.3 Hz), 4.19 (m, 2H), 3.48 (m, 2H), 3.09 (m, 2H), 2.57 (t, 2H, J = 7.2 Hz), 2.53 (s, 2H), 2.19 (s, 3H), 2.17 (s, 3H), 2.09 (s, 3H), 1.76 (m, 2H), 1.63 (s, 6H), 1.48 (m, 4H), 1.43–1.17 (br, 24H), 1.00 (t, 3H, J = 7.2 Hz), 0.90 (m, 3H). ^{13}C NMR (125 MHz, $CDCl_3$) δ: 174.7, 173.8, 164.4, 163.9, 149.7, 149.6, 138.4, 136.6, 134.0, 132.3, 132.0, 130.6, 129.3, 126.8, 124.2, 122.8, 122.3, 119.9, 109.3, 102.6, 49.4, 46.0, 40.0, 39.5, 38.0, 34.7, 31.8, 31.5, 29.9, 29.2, 29.2, 29.2, 29.2, 29.1, 29.0, 28.9, 28.8, 28.7, 24.8, 24.2, 22.2, 20.0, 19.6, 13.7, 13.5.

*4.2.49. 2-(2-hydroxycarbonyl-1,1-dimethylethyl)-3,5-dimethylphenyl stearate/Nap-NH_2 conjugate **8g***

Starting from 250 mg (0.390 mmol) of active ester **7g**, 260 mg (0.330 mmol, 84%) of product **8g** was obtained as a yellow solid.

^{1}H NMR (500 MHz, $CDCl_3$) δ: 8.59 (s, 1H, J = 7.3 Hz), 8.44 (d, 1H, J = 7.6 Hz), 8.25 (d, 1H, J = 8.2 Hz), 7.65 (t, 1H, J = 7.8 Hz), 7,06 (br, 1H), 6.54 (s, 1H), 6.50 (s, 1H), 6.45 (s, 1H, J = 8.4 Hz), 6.28 (t, 1H, J = 6.1 Hz), 4.19 (m, 2H), 3.47 (m, 2H), 3.09 (m, 2H), 2.57 (t, 2H, J = 7.2 Hz), 2.53 (s, 2H), 2.19 (s, 3H), 2.17 (s, 3H), 2.09 (s, 3H), 1.74 (m, 2H), 1.63 (s, 6H), 1.48 (m, 4H), 1.45–1.15 (br, 28H), 0.99 (t, 3H, J = 7.4 Hz), 0.90 (m, 3H). ^{13}C NMR (125 MHz, $CDCl_3$) δ: 175.2, 174.2, 164.8, 164.3, 150.2, 150.0, 138.8, 137.1, 134.5, 132.7, 132.5, 131.1, 129.8, 127.3, 124.7, 123.3, 122.8, 120.4, 109.8, 103.1, 49.9, 46.5, 40.4, 40.0, 38.5, 35.2, 32.3, 31.9, 30.4, 29.7, 29.67 29.7, 29.6, 29.4, 29.4, 29.2, 29.2, 25.3, 24.7, 22.7, 20.5, 20.1, 14.1, 13.9.

4.3. Microorganisms and growth conditions

The reference strains used in this study were: *Candida albicans* ATCC 10231, *Candida glabrata* DSM 11226, *Candida krusei* DSM 6128, *Candida parapsilosis* DSM 5784, *Candida guiliermondi* DSM 11947, *Candida famata* DSM 3428, *Candida rugose* DSM 2031, *Candida pseudotropicalis* KKP 324. Strains were grown at 30 °C in YPD medium (2% glucose, 1% Yeast Extract, and 1% Bacto Peptone) and stored on YPD agar plates

Table 2
Retention times and MS peaks used to identify compounds by HPLC-MS analysis of samples collected from reaction mixtures during enzymatic cleavage of conjugates **6a-g**.

		digested conjugate			5-fluorocytosine			byproduct C		
	Gradient profile	rt (min)	$[M+H]^+$ calc.	$[M+H]^+$ meas.	rt (min)	$[M+H]^+$ calc.	$[M+H]^+$ meas.	rt (min)	$[M+H]^+$ calc.	$[M+H]^+$ meas.
6a	I	17.6	376.2	376.0	1.5	130.0	129.9	20.5	205.1	205.1
6b	II	28.3	460.3	460.1	1.6		129.9	24.3		205.0
6c	II	29.8	488.3	488.1	1.7		129.9	24.3		205.0
6d	II	31.3	516.3	516.2	1.7		129.9	24.3		205.0
6e	II	32.0	544.2	544.3	1.7		129.9	24.2		204.9
6f	III	21.0	572.4	572.3	1.6		129.8	–		–
6g	III	28.9	600.4	600.4	1.5		129.9	–		–

containing 2% agar.

4.4. Determination of antifungal in vitro activity

The *in vitro* growth inhibitory activity of antifungals was quantified by determination of MIC values by the serial two-fold dilution method, using the 96-well microtiter plates, in RPMI-1640 medium w/o sodium bicarbonate, with L-glutamine +2% glucose +3.45% MOPS, pH adjusted to 7.0. Serial dilutions of compounds tested were prepared in the 512–1 μg mL^{-1} range for conjugates testing and in the 64–0.125 μg mL^{-1} range for 5-FC testing. Conditions of the assay were the same as outlined in the CLSI recommendations.

4.5. Hemolysis assay

Red blood cell concentrates were kindly provided by the Regional Center for Blood Donation and Blood Treatment in Gdańsk. The hemolytic activity determination was carried out by the serial dilution method. Briefly, human erythrocytes were suspended in saline to give a suspension of 2×10^7 cells mL^{-1} (hemocytometer count). The stock 1 mg mL^{-1} solutions of conjugates were prepared in DMSO and 50 μL aliquots of serial two-fold dilutions were placed in Eppendorf tubes. Tubes containing 50 μL of DMSO and 50 μL of 2% aqueous Triton X-100 solution were included as a negative and positive control, respectively. To each tube, 950 μL of the erythrocyte suspension was added and mixed by inversion to give the final concentrations of compounds tested in the 200–0.4 μg mL^{-1} range. The samples were incubated at 37 °C for 30 min, then were mixed by inversion and centrifuged (1700×*g*, 5 min, 4 °C). The concentration of hemoglobin in supernatants obtained after the centrifugation of erythrocytes suspension was determined by measuring the absorbance at wavelength λ = 540 nm ($A_{540}{}^{sample}$). Absorbance of the negative ($A_{540}{}^{DMSO}$) and the positive ($A_{540}^{0.1\%Triton\ X-100}$) controls was also measured. The percent of hemolysis at a given compound concentration/EH (%)/was calculated as follows:

$$EH\ (\%) = ((A_{540}^{sample} - A_{540}^{DMSO})/(A_{540}^{0.1\%Triton\ X-100} - A_{540}^{DMSO})) \times 100$$

The EH_{50} values for each compound were calculated with the GraphPad Prism software as an interpolated concentration of compound, for which the A_{540} value is exactly 50% of the A_{540} value measured for the positive control sample.

4.6. Determination of esterase-driven cleavage

Enzymatic reaction. Stock 10 mM solutions of a given compound in methanol were diluted 20-fold with distilled water. To a 10 mL of thus obtained mixture, 12.5 units of pig liver esterase dissolved in a minimal volume of water was added. The enzymatic reaction was performed at the ambient temperature, with magnetic stirring. Samples of 1 mL were collected 1, 15, 30, 45, 60, 90 and 120 min after enzyme addition. A sample of the incubation mixture collected before enzyme addition was used as a negative control. Each sample was then diluted 1:1 with methanol, heated to 90 °C for 5 min to inactivate the enzyme, cooled to ambient temperature and then subjected to HPLC-MS analysis.

HPLC analysis. The HPLC-DAD-MS system consisted of a liquid chromatograph, degasser, a binary pump, an auto-sampler, which was combined with an diode array detector (DAD) and MS detector with electrospray source and quadrupole analyser (1260 Infinity II and 6470 Triple Quad LC/MS, Agilent Technologies). The MassHunter software was used to control the LC system for data processing. Chromatographic separation were performed on an Eclipse XDB-C18 column (150 mm × 4.6 mm, 5 μm). For the separations, a gradient of mobile phase A (0.01% HCOOH in H_2O) and mobile phase B (MeOH) was used. Depending on the substance (see Table above) one of the following gradient profiles were used: I) 0 min - 5% mobile phase B, 24 min–100% mobile phase B, 24.5 min–5% mobile phase B, 30 min–5% mobile phase B; II) 0 min - 5% mobile phase B, 30 min–100% mobile phase B, 31 min–5% mobile phase B, 36 min–5% mobile phase B; III) 0 min - 5% mobile phase B, 30 min–100% mobile phase B, 25 min–5% mobile phase B, 30 min–100% mobile phase B; 31 min–5% mobile phase B; 36 min–5% mobile phase B. For each separation, the flow rate was 1 mL min^{-1}, the column temperature was 20 °C, and the injection volume was 40 μL. The electrospray source operated in a positive mode. The MS data were collected in a scan mode within the range 100–650 *m/z*, scan time of 2.36 cycles/s and fragmentor at 135 V. The DAD data were collected at $\lambda = 254$ nm.

For each separation, peaks of three compounds were identified: the digested conjugate (**6a-g**), 5-fluorocytosine (**5-FC**) and the byproduct of TML linker decomposition (**C**). Each compound for each chromatogram had its identity confirmed by the analysis of MS spectra which were collected during separation (Table 2).

4.7. Microscopic examination of conjugate uptake

Candida cells from the overnight culture in YPD medium were harvested, washed with distilled water and used for inoculation of RPMI-1640 medium. The culture was grown at 30 °C with shaking from $OD_{660} = 0.1$ to $OD_{660} = 0.3$. The cells were harvested by centrifugation and immediately suspended in PBS to $OD_{660} = 0.2$. A conjugate containing fluorescent probe (**8a-g**) was added to the final concentration of 50 μg mL^{-1} and the cell suspension was incubated (30 °C, 150 rpm). Samples of 2 mL were collected at zero time and at time intervals, centrifuged and washed 4 times with PBS. After the final wash, the cells were suspended in a small volume of PBS and immediately observed using the confocal microscopy (63× magnification; ZEISS LSM T-PMT, Magdeburg, Germany). The imaging conditions were as follows: excitation 438 nm, emission 527 nm.

Author contributions

All authors have given approval to the final version of the manuscript.

Funding

This research was funded in whole by the National Science Centre,

Poland under the UMO-2020/39/B/ST4/01509 grant.

Declaration of competing interest

The authors declare the following financial interests/personal relationships which may be considered as potential competing interests: Slawomir Milewski reports financial support was provided by National Science Centre Poland.

Data availability

The data presented in this study are openly available from 1 August 2022 in https://mostwiedzy.pl/pl/open-research-data at doi: 10.34808/676d-re51.

Acknowledgements

The authors acknowledge a substantial support of Dr. Katarzyna Kozłowska-Tylingo, PhD in HPLC-MS analyses. The FOSTER Foundation is gratefully acknowledged for the opportunity to perform experiments on Zeiss LSM T-PMT Confocal Laser Scanning Microscope and 1260 Infinity II, 6470 Triple Quad LC/MS and Teledyne CombiFlash Nextgen 300+ flash chromatography system.

Appendix A. Supplementary data

Supplementary data to this article can be found online at https://doi.org/10.1016/j.ejmech.2023.115293.

References

[1] S. Davies, J. Grant, M. Catchpole, The Drugs Don't Work: A Global Threat, Penguin Books Ltd., London, 2013.
[2] B. Spellberg, The future of antibiotics, Crit. Care 18 (2014) 228.
[3] G.D. Brown, D.W. Denning, N.A.R. Gow, S.M. Levitz, M.G. Netea, T.C. White, Hidden killers: human fungal infections, Sci. Transl. Med. 4 (2012) 1–10.
[4] F. Almeida, M.J. Rodrigues, C. Coelho, The still underestimated problem of fungal diseases worldwide, Front. Microbiol. 10 (2019) 214.
[5] S.E. Jacobs, P. Zagaliotis, T.J. Walsh, Novel antifungal agents in clinical trials, F1000Res 10 (2021) 507.
[6] A.V. Cheng, W.M. Wuest, Signed, sealed, delivered: conjugate and prodrug strategies as targeted delivery vectors for antibiotics, ACS Infect. Dis. 5 (2019) 816–828.
[7] A.S. Skwarecki, S. Milewski, M. Schielmann, M.J. Milewska, Antimicrobial molecular nanocarrier–drug conjugates, Nanomedicine 12 (2016) 2215–2240.
[8] A. Chrzanowska, M. Struga, P. Roszkowski, M. Koliński, S. Kmiecik, K. Jałbrzykowska, A. Zabost, J. Stefańska, E. Augustynowicz-Kopeć, M. Wrzosek, A. Bielenica, The effect of conjugation of Ciprofloxacin and Moxifloxacin with fatty acids on their antibacterial and anticancer activity, Int. J. Mol. Sci. 23 (2022) 6261.
[9] A.R. Waldorf, A. Polak, Mechanisms of action of 5-fluorocytosine, Antimicrob. Agents Chemother. 23 (1983) 79–85.
[10] M.A. Pfaller, S.A. Messer, L. Boyken, H. Huynh, R.J. Hollis, D.J. Djekema, *In vitro* activities of 5-fluorocytosine against 8803 clinical isolates of Candida spp.: global assessment of primary resistance using National Committee for Clinical Laboratory Standards susceptibility testing methods. Antimicrob, Agents Chemother 46 (2002) 3518–3521.
[11] A. Vermes, H.J. Guchelaar, J. Dankert, Flucytosine: a review of its pharmacology, clinical indications, pharmacokinetics, toxicity and drug interactions, J. Antimicrob. Chemother. 46 (2000) 171–179.
[12] F.Z. Delma, A.M.S. Al-Hatmi, R.J.M. Brüggemann, W.J.G. Melchers, S. de Hoog, P. E. Verweij, J.B. Buil, Molecular mechanisms of 5-fluorocytosine resistance in yeasts and filamentous fungi, J. Fungi 7 (2021) 909.
[13] Y.-N. Chen, H.J. Lo, C.C. Wu, H.C. Ko, T.P. Chang, Y.J. Yang, Loss of heterozygosity of *FCY2* leading to the development of flucytosine resistance in *Candida tropicalis*, Antimicrob. Agents Chemother. 55 (2011) 2506–2514.
[14] O.A. Okoh, P. Kahn, Trimethyl lock: a functional molecular tool for drug delivery, cellular imaging, and stimuli-responsive materials, Chembiochem 19 (2018) 1668–1694.
[15] M.J. van Haren, Y. Gao, N. Buijs, R. Campagna, D. Sartini, M. Emanuelli, L. Mateuszuk, A. Kij, S. Chlopicki, P. Escudé Martinez de Castilla, R. Schiffelers, N. I. Martin, Esterase-sensitive prodrugs of a potent bisubstrate inhibitor of nicotinamide N-methyltransferase (NNMT) display cellular activity, Biomolecules 11 (2021) 1357.
[16] C. Ji, M.J. Miller, Chemical syntheses and *in vitro* antibacterial activity of two desferrioxamine B-ciprofloxacin conjugates with potential esterase and phosphatase triggered drug release linkers, Bioorg. Med. Chem. 20 (2012) 3828–3836.
[17] C. Ji, P.A. Miller, M.J. Miller, Syntheses and antibacterial activity of *N*-acylated Ciprofloxacin derivatives based on the trimethyl lock, ACS Med. Chem. Lett. 6 (2015) 707–710.
[18] C. Ji, M.J. Miller, Siderophore–fluoroquinolone conjugates containing potential reduction-triggered linkers for drug release: synthesis and antibacterial activity, Biometals 28 (2015) 541–551.
[19] A.S. Skwarecki, D. Martynow, M.J. Milewska, S. Milewski, Molecular umbrella as a nanocarrier for antifungals, Molecules 26 (2021) 5475.
[20] A. Jaworski, M. Szcześniak, K. Szczepaniak, K. Kubulat, W.P. Person, Infrared spectra and tautomerism of 5-fluorocytosine, 5-bromocytosine and 5-iodocytosine. Matrix isolation and theoretical AB initio studies, J. Mol. Struct. 223 (1990) 63–92.
[21] M.E. Falagas, N. Roussos, K.Z. Vardakas, Relative frequency of albicans and the various non-albicans *Candida* spp. among candidemia isolates from inpatients in various parts of the world: a systematic review, Int. J. Infect. Dis. 14 (2010) 954–966.
[22] Clinical and Laboratory Standards Institute, Reference method for broth dilution antifungal susceptibility testing of yeasts, in: Approved Standard M27-A3, third ed., Clinical and Laboratory Standards Institute, Wayne, PA, USA, 2008.
[23] S.T. Akula, A. Nagaraja, M. Ravikanth, N.G. Raj Kumar, Y. Kalyan, D. Divya, Antifungal efficacy of lauric acid and caprylic acid – derivatives of virgin coconut oil against *Candida albicans*, Biomed. Biotechnol. Res. J 5 (2021) 229–234.
[24] J.G. Allen, F.R. Atherton, M.J. Hall, C.H. Hassall, S.W. Holmes, R.W. Lambert, L. J. Nisbet, P.S. Ringrose, Phosphonopeptides, a new class of synthetic antibacterial agents, Nature 272 (1978) 56–58.
[25] W.D. Kingsbury, J.C. Boehm, R.J. Mehta, S.F. Grappel, Transport of antimicrobial agents using peptide carrier systems: anticandidal activity of *m*-fluorophenylalanine–peptide conjugates, J. Med. Chem. 26 (1983) 1725–1729.
[26] R. Andruszkiewicz, S. Milewski, T. Zieniawa, E. Borowski, Anticandidal properties of N^3-(4-methoxyfumaroyl)-L-2,3-diaminopropanoic acid oligopeptides, J. Med. Chem. 33 (1990) 132–135.
[27] D. Bartee, S. Sanders, P.D. Phillips, M.J. Harrison, A.T. Koppisch, C.L.F. Meyers, Enamide prodrugs of acetyl phosphonate deoxy-D-xylulose-5-phosphate synthase inhibitors as potent antibacterial agents, ACS Infect. Dis. 5 (2019) 406–417.
[28] W.D. Kingsbury, J.C. Boehm, R.J. Mehta, S.F. Grappel, C. Gilvarg, A novel peptide delivery system involving peptidase activated prodrugs as antimicrobial agents. Synthesis and biological activity of peptidyl derivatives of 5-fluorouracil, J. Med. Chem. 27 (1984) 1447–1451.
[29] Q. Jin, F. Mitschang, S. Agarwal, Biocompatible drug delivery system for photo-triggered controlled release of 5-fluorouracil, Biomacromolecules 12 (2011) 3684–3691.